

Polarized and unpolarized off-shell $H^* \rightarrow ZZ \rightarrow 4\ell$ decay above the $2m_Z$ threshold

A. I. Hernández-Juárez,^{1,*} R. Gaitán,¹ and G. Tavares-Velasco²

¹Departamento de Física, FES-Cuautitlán, Universidad Nacional Autónoma de México, C.P. 54770, Estado de México, México.

²Facultad de Ciencias Físico Matemáticas, Benemérita Universidad Autónoma de Puebla, Apartado Postal 1152, Puebla, Puebla, México

(Dated: July 9, 2024)

An analysis of the off-shell $H^* \rightarrow ZZ \rightarrow \bar{\ell}_1\ell_1\bar{\ell}_2\ell_2$ decay width is presented for both unpolarized and polarized Z gauge bosons in the scenario with the most general H^*ZZ vertex function, which is given in terms of two CP -even (\hat{b}_Z and \hat{c}_Z) and one CP -odd (\tilde{b}_Z) anomalous couplings. The SM contributions to the H^*ZZ coupling up to the one-loop level are also included. Explicit analytic results for the unpolarized and polarized $H^* \rightarrow ZZ \rightarrow \bar{\ell}_1\ell_1\bar{\ell}_2\ell_2$ square amplitudes and the four-body phase space are presented, out of which several observable quantities can be obtained straightforwardly. As far as the numerical analysis is concerned, a cross-check is performed via `MadGraph5_aMC@NLO`, where our model was implemented with the aid of `FeynRules`. We then consider the most stringent bounds on anomalous complex H^*ZZ couplings and analyze the effects of the polarizations of the Z gauge bosons through the polarized $H^* \rightarrow ZZ \rightarrow \bar{\ell}_1\ell_1\bar{\ell}_2\ell_2$ decay width as well as left-right and forward-backward asymmetries, which are found to be sensitive to new-physics effects. Particular focus is put on the effects of the absorptive parts of the anomalous H^*ZZ couplings, which have been largely overlooked up to now in LHC analyses. It is found that the studied observable quantities, particularly the left-right asymmetries, can be helpful to look for effects of CP -violation in the H^*ZZ coupling and set bounds on the absorptive parts. For completeness, we also analyze the case of unpolarized Z gauge bosons.

I. INTRODUCTION

All the experimental data collected until now indicate that the properties of the scalar particle discovered in 2012 at the LHC by the ATLAS and CMS collaborations [1, 2] are compatible with those of the long-sought-for Higgs boson, which is the remnant of the mechanism of spontaneous symmetry breaking of the $SU(2)_L \times U(1)_Y$ gauge symmetry in the Glashow-Salam-Weinberg Standard Model (SM). Nonetheless, there are still several couplings of such a particle that remain to be measured with enough accuracy, such as for the $H\bar{b}b$ and $H\mu^-\mu^+$ interactions, whereas other ones are still not yet at the reach of experimental measurement, for instance, the Higgs boson couplings to light fermions, let alone the Higgs boson self couplings. Therefore, the study of the Higgs boson phenomenology is expected to play an important role in probing the SM and the search for any new physics effects in present and future colliders. Along these lines, the Higgs boson couplings to the weak gauge bosons HZZ and HWW , which in the SM arise at the tree level, have long drawn considerable attention both theoretically and experimentally. As far as the HZZ coupling is concerned, it has played a crucial part in the experimental study of the Higgs boson at the LHC via the $H \rightarrow ZZ^* \rightarrow 4\ell$ decay, which provides a clear signal and allows for a precise resolution of the Higgs boson mass despite that its branching ratio is considerably smaller than those of other decay channels such as $H \rightarrow WW^*$, $H \rightarrow \tau^+\tau^-$, and $H \rightarrow \bar{b}b$. A milestone was achieved in 2022 when the CMS collaboration reported for the first time the measurement of the off-shell H^*ZZ coupling via the $pp \rightarrow H^* \rightarrow ZZ$ process [3]. This result was also confirmed by the ATLAS collaboration the following year [4].

Although one-loop corrections to the HZZ vertex were calculated long ago in the framework of the SM [5, 6], more recently a new evaluation was presented [7] that could be more suitable for the recent progress on the theoretical and experimental study of this coupling.

The most general HZZ vertex can be parametrized by an effective Lagrangian given in terms of four coupling constants:

$$\mathcal{L}^{HZZ} = \frac{g}{c_W} m_Z \left[\frac{(1 - a_Z)}{2} H Z_\mu Z^\mu + \frac{1}{2m_Z^2} \left\{ \hat{b}_Z H Z_{\mu\nu} Z^{\mu\nu} + \hat{c}_Z H Z_\mu \partial_\nu Z^{\mu\nu} + \tilde{b}_Z H Z_{\mu\nu} \tilde{Z}^{\mu\nu} \right\} \right], \quad (1)$$

where a_Z stands for the corrections to the SM tree-level coupling via loop contributions or new physics effects, whereas \hat{b}_Z , \hat{c}_Z and \tilde{b}_Z are absent at the tree level in the SM and thus are dubbed anomalous couplings. The anomalous CP -conserving coupling \hat{b}_Z is induced at the one-loop level [5, 6] and can reach values of the order of 10^{-3} [7], while the

* alan.hernandez@cuautitlan.unam.mx

CP -violating one \tilde{b}_Z would arise up to the three-loop level and has been estimated to be of the order of 10^{-11} [8]. The \hat{c}_Z anomalous coupling is also expected to be generated at one-loop level, but it has not been identified in SM calculations.

The phenomenology of the HZZ anomalous couplings have been extensively studied in both lepton [9–11] and hadron colliders [12]. These studies have shown that non-SM contributions to the HZZ coupling could be significantly constrained in the future, providing an opportunity to detect new physics effects through HZZ -mediated processes. In particular, polarization observables in the $Z^* \rightarrow HZ$ process at the LHC have been used to revisit the anomalous couplings, yielding limits of around $10^{-3} - 10^{-4}$ for the real and absorptive parts of the CP -conserving \hat{b}_Z anomalous coupling and of order 10^{-3} for the CP -violating \tilde{b}_Z coupling [13]. Furthermore, limits on the anomalous couplings have been established at various colliders, including e^-e^- , ep , and γe colliders [10, 14–24]. The CMS collaboration has also obtained bounds on effective ratios of the anomalous couplings [3, 25–27], which were combined with the theoretical SM contribution to \hat{b}_Z in a recent study [7]. It was found that the \hat{c}_Z and \tilde{b}_Z anomalous couplings can be constrained to as tight as $10^{-2} - 10^{-4}$ depending on the energy region. Finally, other off-shell couplings such as trilinear neutral gauge boson couplings [28–31] and the coupling of the gluon with a quark-antiquark pair [32, 33] have also been investigated in recent studies.

In this work, we are interested in the study of the HZZ anomalous couplings effects on the off-shell decay $H^* \rightarrow ZZ \rightarrow 4\ell$ via polarized Z gauge bosons. The polarizations of Z boson are of great interest at the LHC, as recently a longitudinally polarized Z boson pair has been reported by the ATLAS collaboration [34], and the production of longitudinally $W^\pm Z$ pairs is also being studied [35]. The polarization fractions of the Z boson have been measured by the CMS, ATLAS and LHCb collaborations [36–39]. Previous analysis of gauge bosons polarization at the LHC include $W^\pm Z$ production [40], $W + \text{Jets}$ events [41, 42], W bosons produced in top decays [43–46], $W^\pm W^\pm$ production [47]. The **MadGraph5_aMC@NLO** [48] and **SHERPA** [49] event generators have also included the possibility of generating polarized amplitudes. A method to identify Z bosons polarizations has been discussed in Ref. [50], whereas a higher sensitivity to polarized Z bosons is also expected in the recent upgrade of the LHC [51]. We will consider the most general scenario with both Z gauge bosons on-shell and complex anomalous HZZ couplings. Furthermore, we will analyze the behavior of some observables that can be sensitive to new physics contributions. In particular, we are interested in the effects of the absorptive parts of the anomalous HZZ couplings, which have been overlooked in the past but can lead to interesting results. For the sake of completeness, we also discuss the scenario with unpolarized Z gauge bosons.

The rest of this work is as follows. Section II is devoted to discuss the theoretical framework appropriate for the study of the $H^* \rightarrow ZZ \rightarrow 4\ell$ decay width, with explicit analytical expressions for the polarized and unpolarized square amplitudes, out of which the respective $H^* \rightarrow ZZ \rightarrow 4\ell$ differential decay widths are obtained. The numerical analysis is presented in Sec. III, where we cross-check our calculation method with an alternative evaluation performed via **MadGraph5_aMC@NLO**. The behavior of the differential decay, angular distributions along with left-right and a forward-backward asymmetries are analyzed in some realistic scenarios for the values of the real and absorptive parts of the anomalous HZZ couplings. In Section IV we present our concluding remarks and outlook. Finally, the kinematics of the $H^* \rightarrow ZZ \rightarrow 4\ell$ decay and the four-body phase space are discussed in Appendix A.

II. POLARIZED AND UNPOLARIZED $H^* \rightarrow \bar{\ell}_1\ell_1\bar{\ell}_2\ell_2$ DECAY WIDTHS

We now present all the analytical formulas required for the calculation of the unpolarized and polarized $H^* \rightarrow \bar{\ell}_1\ell_1\bar{\ell}_2\ell_2$ decay width. The most general form of the HZZ vertex functions with complex anomalous couplings is considered, whereas the contributions of the SM up to the one-loop level are also included [7].

A. HZZ vertex function

The S -matrix element obtained from Lagrangian (1) can be written as

$$i\mathcal{M} = i \frac{g}{c_W} m_Z \Gamma_{\mu\nu}^{ZZH}(q^2) Z^\mu(p_1) Z^\nu(p_2) H(q), \quad (2)$$

where the vertex function $\Gamma_{\mu\nu}^{ZZH}(q^2)$ can be written as follows for on-shell Z gauge bosons and an off-shell Higgs boson

$$\Gamma_{\mu\nu}^{ZZH}(q^2) = h_1^H(q^2) g_{\mu\nu} + \frac{h_2^H(q^2)}{m_Z^2} p_{1\nu} p_{2\mu} + \frac{h_3^H(q^2)}{m_Z^2} \epsilon_{\mu\nu\alpha\beta} p_1^\alpha p_2^\beta, \quad (3)$$

with h_i^H ($i = 1, 2, 3$) the form factors that are given in terms of the anomalous couplings of Lagrangian (1) as follows

$$h_1^H(q^2) = 1 + a_Z - \hat{b}_Z \frac{q^2 - 2m_Z^2}{m_Z^2} + \hat{c}_Z, \quad (4)$$

$$h_2^H(q^2) = \pm 2\hat{b}_Z, \quad (5)$$

$$h_3^H(q^2) = \pm 2\tilde{b}_Z. \quad (6)$$

These form factors are both explicit and implicit functions of q^2 since the anomalous couplings also depend on the off-shell Higgs boson four-momentum.

As the main interest of this work is the study of the anomalous contributions, we will consider a vanishing a_Z . For a study of the SM one-loop contributions to the a_Z coupling along with the renormalization procedure, we refer the reader to Ref. [5]. The \hat{b}_Z , \hat{c}_Z and \tilde{b}_Z anomalous couplings will be considered as non-zero in the rest of this work. This is feasible in the SM, and new physics contributions from new particles can also arise under the context of the two-Higgs doublet and Higgs singlet models [52], the minimal Higgs triplet model [53] and the minimal supersymmetric SM [54]. Recently, the SMEFT contributions have also been revisited [24]. Additionally, the CP -violating \tilde{b}_Z anomalous coupling may be induced through flavor changing neutral currents mediated by the Z or H bosons, as in the $HZ\gamma$ vertex [55].

Since the anomalous couplings can be taken as complex in general [7, 56], the form factors of (4)-(6) will be written as follows

$$h_i^H = \text{Re}[h_i^H] + i\text{Im}[h_i^H]. \quad (7)$$

Before moving forward, it is important to note a few general limitations regarding the prescription used in Lagrangian (1) and the absorptive parts of the form factors. It is observed that the HZZ Lagrangian requires real \hat{b}_Z , \hat{c}_Z and \tilde{b}_Z anomalous couplings to be Hermitian. This seems to contradict our assumption in Eq. (7). However, the Lagrangian (1) is only valid in the Born approximation as it exclusively describes the external particles in an effective approach [57]. On the other hand, anomalous couplings are generated through quantum corrections by heavy or light particles at one-loop level or higher orders. The new operators that induce these loop effects are not accounted for in Lagrangian (1) and do not necessarily necessitate real anomalous couplings to form Hermitian amplitudes [9]. For instance, in the SM, the contributions arising at the one-loop level develop an absorptive part as long as the magnitude of the off-shell Higgs boson four-momentum is above the $\|q\| = 2m_i$ threshold, where m_i is the mass of the particles coupled to H . Therefore, in the most general scenario, the \hat{b}_Z , \hat{c}_Z , and \tilde{b}_Z anomalous couplings are no longer real constants but complex functions of q^2 . This general scenario is the one we will consider in our analysis.

Although the absorptive parts have been neglected in experimental analyses at the LHC, their effects have been discussed in some theoretical works [9, 13, 15] and more recently via a left-right asymmetry [7], which may be reconstructed in the final state of the $H^* \rightarrow ZZ \rightarrow \bar{\ell}_1 \ell_1 \bar{\ell}_2 \ell_2$ decay. Polarization effects of the Z gauge bosons on the Higgs boson decay $H \rightarrow ZZ$ have already been studied [58, 59], though only non-anomalous HZZ couplings and one on-shell Z gauge boson were considered. Similar calculations were also reported in [8, 60–62]. On the other hand, the scenario where both Z gauge bosons are on-shell and the HZZ coupling is purely real was studied in Refs. [6, 63, 64]. Finally, a restrictive scenario where not all the HZZ anomalous couplings were taken as complex was considered in Ref. [15].

In this work, we are interested in the most general scenario where all the anomalous HZZ couplings are complex and calculate the unpolarized and polarized off-shell $H^* \rightarrow ZZ \rightarrow \bar{\ell}_1 \ell_1 \bar{\ell}_2 \ell_2$ decay width. We will then analyze the implications of the absorptive parts of the HZZ anomalous couplings on some observables.

B. Polarized Amplitudes

Using the nomenclature of Fig. 1, the amplitude for the $H^* \rightarrow Z(p_1)Z(p_2) \rightarrow \bar{\ell}_1 \ell_1 \bar{\ell}_2 \ell_2$ process can be written as

$$\mathcal{M}_{H^* \rightarrow \bar{\ell}_1 \ell_1 \bar{\ell}_2 \ell_2} = \mathcal{M}_{H^* \rightarrow Z(p_1)Z(p_2)}^{\mu\nu} \frac{i \sum \epsilon_\eta(p_1, \lambda_1) \epsilon_\mu^*(p_1, \lambda_1)}{p_1^2 - m_Z^2 + i\Gamma_Z m_Z} \mathcal{M}_{Z(p_1) \rightarrow \bar{\ell}_1 \ell_1}^\eta \frac{i \sum \epsilon_\kappa(p_2, \lambda_2) \epsilon_\nu^*(p_2, \lambda_2)}{p_2^2 - m_Z^2 + i\Gamma_Z m_Z} \mathcal{M}_{Z(p_2) \rightarrow \bar{\ell}_2 \ell_2}^\kappa, \quad (8)$$

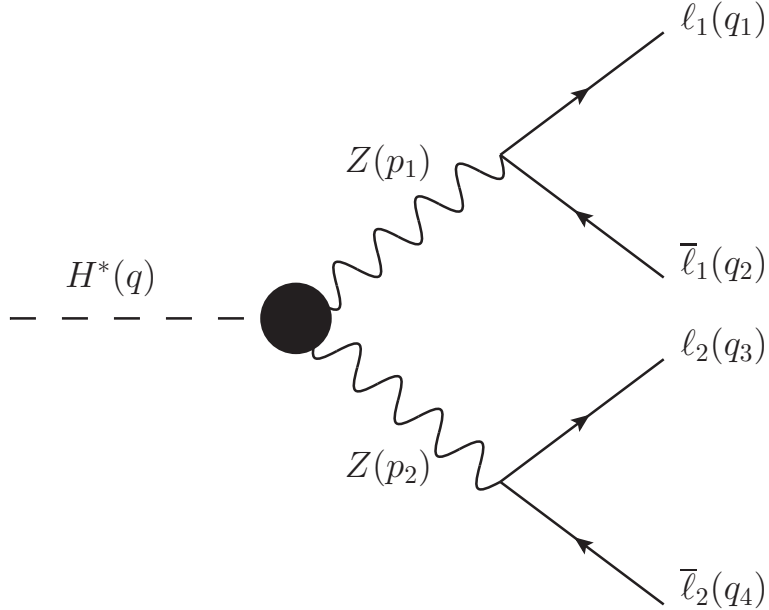


FIG. 1. Nomenclature for the four-momenta of the particles involved in the Feynman diagram for the contribution of the HZZ anomalous couplings to the Higgs boson decay $H^* \rightarrow Z(p_1)Z(p_2) \rightarrow \bar{\ell}_1\ell_1\bar{\ell}_2\ell_2$.

where Γ_Z is the Z gauge boson decay width, and, according to Lagrangian (1), the amplitude for the process $H^* \rightarrow ZZ$ is given in terms of the complex h_i^H form factors as follows

$$\begin{aligned} \mathcal{M}_{H^* \rightarrow Z(p_1)Z(p_2)}^{\mu\nu} = & i \left(\frac{g}{c_W} \right) m_Z \left\{ g^{\mu\nu} \left(\text{Re}[h_1^H] + i\text{Im}[h_1^H] \right) + \frac{p_2^\mu p_1^\nu}{m_Z^2} \left(\text{Re}[h_2^H] + i\text{Im}[h_2^H] \right) \right. \\ & \left. + \frac{\epsilon^{\mu\nu\alpha\beta} p_{1\alpha} p_{2\beta}}{m_Z^2} \left(\text{Re}[h_3^H] + i\text{Im}[h_3^H] \right) \right\}, \end{aligned} \quad (9)$$

whereas the amplitudes for the $Z \rightarrow \bar{\ell}_1\ell_1$ and $Z \rightarrow \bar{\ell}_2\ell_2$ processes are

$$\mathcal{M}_{Z(p_1) \rightarrow \bar{\ell}_1\ell_1}^\eta = i \frac{g}{c_W} \bar{u}(q_2) \gamma^\eta (g_V - g_A \gamma^5) u(q_1), \quad (10)$$

$$\mathcal{M}_{Z(p_2) \rightarrow \bar{\ell}_2\ell_2}^\kappa = i \frac{g}{c_W} \bar{u}(q_4) \gamma^\kappa (g_V - g_A \gamma^5) u(q_3). \quad (11)$$

For the Z gauge boson propagators of Eq. (8) we have used the completeness relation [49]

$$-g^{\mu\nu} + \frac{k^\mu k^\nu}{m_Z^2} = \sum_{\lambda=1}^3 \epsilon_\lambda^\mu(k) \epsilon_\lambda^{*\nu}(k), \quad (12)$$

where we only consider 3 polarizations since both Z gauge bosons are on-shell.

In order to study the polarization effects in the final state, it is convenient to rewrite Eq. (8) as a sum of the polarized amplitudes

$$\mathcal{M}_{H^* \rightarrow \bar{\ell}_1\ell_1\bar{\ell}_2\ell_2}(\lambda_1, \lambda_2) = \sum_{\lambda_1} \sum_{\lambda_2} \frac{\mathcal{M}_{H^* \rightarrow Z(p_1)Z(p_2)}(\lambda_1, \lambda_2) \mathcal{M}_{Z(p_1) \rightarrow \bar{\ell}_1\ell_1}(\lambda_1) \mathcal{M}_{Z(p_2) \rightarrow \bar{\ell}_2\ell_2}(\lambda_2)}{(p_1^2 - m_Z^2 + i\Gamma m_Z)(p_2^2 - m_Z^2 + i\Gamma m_Z)} \quad (13)$$

where

$$\mathcal{M}_{H^* \rightarrow Z(p_1)Z(p_2)}(\lambda_1, \lambda_2) = \mathcal{M}_{H^* \rightarrow Z(p_1)Z(p_2)}^{\mu\nu} \epsilon_\mu^*(p_1, \lambda_1) \epsilon_\nu^*(p_2, \lambda_2), \quad (14)$$

$$\mathcal{M}_{Z(p_i) \rightarrow \bar{\ell}_i\ell_i}(\lambda_i) = \mathcal{M}_{Z(p_i) \rightarrow \bar{\ell}_i\ell_i}^\mu \epsilon_\mu(p_i, \lambda_i). \quad (15)$$

Since the $\mathcal{M}_{H^* \rightarrow Z(p_1)Z(p_2)}(\lambda_1, \lambda_2)$ polarized amplitude is non-vanishing for $\lambda_1 = \lambda_2$ only [7, 64], the square amplitude can be written as

$$\mathcal{M}_{H^* \rightarrow \bar{\ell}_1 \ell_1 \bar{\ell}_2 \ell_2}^2 = \frac{\sum_{\lambda} \mathcal{M}_{H^* \rightarrow Z(p_1)Z(p_2)}^2(\lambda, \lambda) \mathcal{M}_{Z(p_1) \rightarrow \bar{\ell}_1 \ell_1}^2(\lambda) \mathcal{M}_{Z(p_2) \rightarrow \bar{\ell}_2 \ell_2}^2(\lambda) + \mathcal{M}_{\text{int}}^2}{((p_1^2 - m_Z^2)^2 + \Gamma^2 m_Z^2) ((p_2^2 - m_Z^2)^2 + \Gamma^2 m_Z^2)}. \quad (16)$$

where the interference term $\mathcal{M}_{\text{int}}^2$ is given by

$$\begin{aligned} \mathcal{M}_{\text{int}}^2 = & \sum_{\lambda_1} \sum_{\lambda_2 \neq \lambda_1} \mathcal{M}_{H^* \rightarrow Z(p_1)Z(p_2)}(\lambda_1, \lambda_1) \mathcal{M}_{H^* \rightarrow Z(p_1)Z(p_2)}^\dagger(\lambda_2, \lambda_2) \mathcal{M}_{Z(p_1) \rightarrow \bar{\ell}_1 \ell_1}(\lambda_1) \mathcal{M}_{Z(p_1) \rightarrow \bar{\ell}_1 \ell_1}^\dagger(\lambda_2) \\ & \times \mathcal{M}_{Z(p_2) \rightarrow \bar{\ell}_2 \ell_2}(\lambda_1) \mathcal{M}_{Z(p_2) \rightarrow \bar{\ell}_2 \ell_2}^\dagger(\lambda_2). \end{aligned} \quad (17)$$

From the first term of the right-hand side of Eq. (16) we can extract the contributions of polarized Z gauge bosons with polarizations $\lambda = L, R$, and 0, which allows one to study the polarized decay width and other observables of interest. As described below, to obtain the $H^* \rightarrow \bar{\ell}_1 \ell_1 \bar{\ell}_2 \ell_2$ decay width we will follow the approach of Ref. [60] for the calculation of the $H \rightarrow ZZ^* \rightarrow \bar{\ell}_1 \ell_1 \bar{\ell}_2 \ell_2$ decay. A similar procedure was followed in Ref. [65, 66] for the decay $K^\pm \rightarrow \pi^\pm \pi^0 e^+ e^-$, whereas an alternative method was implemented in Ref. [61] for the $H \rightarrow ZZ^* \rightarrow \ell^+ \ell^- \tau^+ \tau^-$ and $H \rightarrow WW^* \rightarrow \ell^- \bar{\nu}_\ell \tau^+ \nu_\tau$ decays using transformation properties of the helicity amplitudes under the rotation group.

The phase space for the $H^* \rightarrow \bar{\ell}_1 \ell_1 \bar{\ell}_2 \ell_2$ process, along with the kinematics, is presented in Appendix A. The relevant angular variables on which the square $\mathcal{M}_{H^* \rightarrow \bar{\ell}_1 \ell_1 \bar{\ell}_2 \ell_2}^2$ amplitude depends are θ_1 , θ_2 and ϕ , which are described in Fig 2. We note that the square polarized amplitudes $\mathcal{M}_{H^* \rightarrow ZZ}^2(\lambda_1, \lambda_2)$, $\mathcal{M}_{Z(p_1) \rightarrow \bar{\ell}_1 \ell_1}^2(\lambda_1)$ and $\mathcal{M}_{Z(p_2) \rightarrow \bar{\ell}_2 \ell_2}^2(\lambda_2)$ can be computed in the corresponding H^* , $Z(p_1)$ and $Z(p_2)$ rest frames since each one depends only on scalar products of four-momenta given in the same inertial frame. Even more, these square amplitudes are Lorentz invariant and it is not necessary to apply a boost to bring them into a common reference system. On the other hand, the interference term $\mathcal{M}_{\text{int}}^2$ is given in terms of partial amplitudes evaluated in distinct reference frames, so a boost from the $Z(p_i) \rightarrow \bar{\ell}_i \ell_i$ reference frames into the Higgs boson rest frame will be required to perform the sum of Eq. (17). The same is true for the calculation of the unpolarized case via standard techniques as scalar products of four-momenta given in distinct reference frames are also involved.

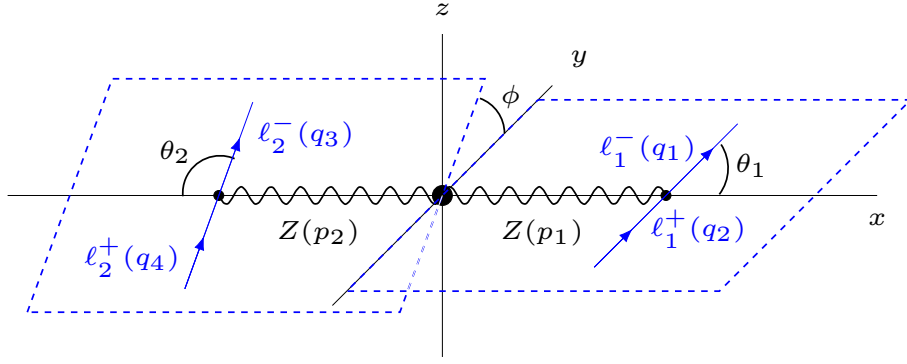


FIG. 2. Nomenclature for the reference systems and angles used in the calculation of the $H \rightarrow ZZ \rightarrow \bar{\ell}_1 \ell_1 \bar{\ell}_2 \ell_2$ decay, as described in Appendix A.

We present below the analytical expressions for the polarized square amplitudes and the interference term of Eq. (16), which were calculated using the FeynCalc package [67–69]. The relation $p_i^2 = m_Z^2$ ($i = 1, 2$) will be considered as the energy region where both Z gauge bosons are on-shell is of interest for our analysis.

1. Polarized $H^* \rightarrow Z(p_1)Z(p_2)$ square amplitudes

The polarized square amplitudes $\mathcal{M}_{H^*}^2(\lambda, \lambda)$ given in terms of the real and absorptive parts of the complex anomalous couplings h_i^H of Lagrangian (1) were presented by some of us in a previous work [7]. We consider a reference frame in which the motion of the $Z(p_1)$ gauge boson is along the positive direction of the x axis and the off-shell Higgs boson is at rest. For further details see Appendix A. In the energy region where both Z gauge bosons are on-shell, the transversally polarized $H^* \rightarrow ZZ$ amplitudes read as follows

$$\mathcal{M}_{H^* \rightarrow Z(p_1)Z(p_2)}^2(L, L) = \left(\frac{g}{2c_W m_Z} \right)^2 \left(4m_Z^2 Q \sqrt{Q^2 - 4m_Z^2} \operatorname{Im} \left(h_3^H h_1^{H\dagger} \right) + Q^2 (Q^2 - 4m_Z^2) |h_3^H|^2 + 4m_Z^4 |h_1^H|^2 \right), \quad (18)$$

and

$$\mathcal{M}_{H^* \rightarrow Z(p_1)Z(p_2)}^2(R, R) = \left(\frac{g}{2c_W m_Z} \right)^2 \left(-4m_Z^2 Q \sqrt{Q^2 - 4m_Z^2} \operatorname{Im} \left(h_3^H h_1^{H\dagger} \right) + Q^2 (Q^2 - 4m_Z^2) |h_3^H|^2 + 4m_Z^4 |h_1^H|^2 \right), \quad (19)$$

whereas for the longitudinal polarization we obtain

$$\begin{aligned} \mathcal{M}_{H^* \rightarrow Z(p_1)Z(p_2)}^2(0, 0) = & \left(\frac{g}{4c_W m_Z^3} \right)^2 \left(4Q^6 m_Z^2 \left(\operatorname{Re} \left(h_1^H h_2^{H\dagger} \right) - 2|h_2^H|^2 \right) + 4Q^4 m_Z^4 \left(|h_1^H|^2 + 4|h_2^H|^2 - 6\operatorname{Re} \left(h_1^H h_2^{H\dagger} \right) \right) \right. \\ & \left. - 16Q^2 m_Z^6 \left(|h_1^H|^2 - 2\operatorname{Re} \left(h_1^H h_2^{H\dagger} \right) \right) + 16m_Z^8 |h_1^H|^2 + Q^8 |h_2^H|^2 \right), \end{aligned} \quad (20)$$

where we have introduced the four-lepton invariant mass $Q^2 = q^2$, instead of the four-momentum of the off-shell Higgs boson. Moreover, we use $\operatorname{Re} \left(h_i^H h_j^{H\dagger} \right) = \operatorname{Re} [h_i] \operatorname{Re} [h_j] + \operatorname{Im} [h_i] \operatorname{Im} [h_j]$ and $\operatorname{Im} \left(h_i^H h_j^{H\dagger} \right) = \operatorname{Im} [h_i] \operatorname{Re} [h_j] - \operatorname{Re} [h_i] \operatorname{Im} [h_j]$. Our results reproduce those reported in Ref. [64] for the scenario with real anomalous couplings.

Note that there is no dependence on the angular variables. Also, a non-vanishing h_3^H form factor may give rise to a left-right asymmetry in the four-lepton final state, which vanishes up to the one-loop level in the SM.

2. $Z(p_i) \rightarrow 2\ell_i$ square amplitudes

As already mentioned, the square amplitudes $\mathcal{M}_{Z(p_1) \rightarrow \bar{\ell}_1 \ell_1}^2(\lambda)$ and $\mathcal{M}_{Z(p_2) \rightarrow \bar{\ell}_2 \ell_2}^2(\lambda)$ can be worked out in the rest frame of the $Z(p_i)$ gauge boson. According to the kinematics presented in Appendix A, the polarization vectors of the $Z(p_1)$ ($Z(p_2)$) gauge boson are oriented along the positive (negative) direction of the x axis, thus the transversally and longitudinally polarized amplitudes are given as

$$\begin{aligned} \mathcal{M}_{Z(p_i) \rightarrow \bar{\ell}_i \ell_i}^2(R/L) = & \left(\frac{g}{c_W} \right)^2 \left(s_{\theta_i}^2 (4m_i^2 - m_Z^2) (g_A^2 + g_V^2) \pm 4g_A g_V c_{\theta_i} m_Z \sqrt{m_Z^2 - 4m_i^2} + 2m_Z^2 (g_A^2 + g_V^2) - 8m_i^2 g_A^2 \right) \\ \simeq & \left(\frac{g}{c_W} \right)^2 m_Z^2 ((g_A^2 + g_V^2) (1 + c_{\theta_i}^2) \pm 4g_A g_V c_{\theta_i}), \end{aligned} \quad (21)$$

and

$$\begin{aligned} \mathcal{M}_{Z(p_i) \rightarrow \bar{\ell}_i \ell_i}^2(0) = & 2 \left(\frac{g}{c_W} \right)^2 (c_{\theta_i}^2 (4m_i^2 - m_Z^2) (g_A^2 + g_V^2) + m_Z^2 (g_A^2 + g_V^2) - 4m_i^2 g_A^2) \\ \simeq & 2 \left(\frac{g}{c_W} \right)^2 s_{\theta_i}^2 m_Z^2 (g_A^2 + g_V^2), \end{aligned} \quad (22)$$

where $i = 1, 2$ and we have introduced the short-hand notation $c_\eta \equiv \cos \eta$ and $s_\eta \equiv \sin \eta$. The approximate results were obtained in the massless lepton limit, which is used in the phase space defined in Appendix A.

To cross-check our calculation, we have boosted Eqs. (21) and (22) into the Higgs boson rest frame via the Lorentz transformation given in Appendix A, which leaves them invariant as expected. We also note that the above square amplitudes are independent of the ϕ angle and the four-lepton invariant mass Q . Also, although the $g_A g_V$ term in Eq. (21) seems to give rise to a left-right asymmetry, it vanishes after integration over the θ_i angles. Therefore, the only observable effects of the left- and right-handed polarized $Z(p_i) \rightarrow \bar{\ell}_i \ell_i$ amplitudes would appear via either angular distributions or a forward-backward asymmetry.

3. Interference term

For the purpose of our work, it is enough to consider the massless lepton approximation, which yields

$$\begin{aligned} \mathcal{M}_{\text{int}}^2 &\equiv \sum_{\lambda_1} \sum_{\lambda_2 \neq \lambda_1} \mathcal{M}_{H^* Z(p_1) Z(p_2)}^2(\lambda_1, \lambda_2) \\ &= \frac{s_{\theta_1} s_{\theta_2}}{2m_Z^2} \left(s_{\theta_1} s_{\theta_2} m_Z^2 (g_A^2 + g_V^2)^2 f_1(Q^2) + (2g_A g_V + c_{\theta_1} (g_A^2 + g_V^2)) (2g_A g_V + c_{\theta_2} (g_A^2 + g_V^2)) f_2(Q^2) \right. \\ &\quad \left. + (2g_A g_V - c_{\theta_1} (g_A^2 + g_V^2)) (2g_A g_V - c_{\theta_2} (g_A^2 + g_V^2)) f_3(Q^2) \right), \end{aligned} \quad (23)$$

where

$$f_1(Q^2) = 4\sqrt{Q^2(Q^2 - 4m_Z^2)} m_Z^2 \text{Re} \left(h_1^H h_3^{H\dagger} \right) s_{2\phi} + \left(4m_Z^4 |h_1^H|^2 - Q^2(Q^2 - 4m_Z^2) |h_3^H|^2 \right) c_{2\phi}, \quad (24)$$

$$\begin{aligned} f_2(Q^2) &= c_\phi \left((Q^2(Q^2 - 4m_Z^2))^{3/2} \text{Im} \left(h_3^H h_2^{H\dagger} \right) \right. \\ &\quad \left. + 2m_Z^2 \left(\sqrt{Q^2(Q^2 - 4m_Z^2)} (Q^2 - 2m_Z^2) \text{Im} \left(h_3^H h_1^{H\dagger} \right) + (4m_Z^2 - Q^2) Q^2 \text{Re} \left(h_1^H h_2^{H\dagger} \right) \right) \right) \\ &\quad - s_\phi \left((Q^2(Q^2 - 4m_Z^2))^{3/2} \text{Re} \left(h_2^H h_3^{H\dagger} \right) \right. \\ &\quad \left. + 2m_Z^2 \left(\sqrt{Q^2 - 4m_Z^2} (Q^2 - 2m_Z^2) \text{Re} \left(h_1^H h_3^{H\dagger} \right) + (Q^2 - 4m_Z^2) Q^2 \text{Im} \left(h_1^H h_2^{H\dagger} \right) \right) \right) \\ &\quad + 4c_\phi m_Z^4 (2m_Z^2 - Q^2) |h_1^H|^2, \end{aligned} \quad (25)$$

and

$$\begin{aligned} f_3(Q^2) &= c_\phi \left(- (Q^2(Q^2 - 4m_Z^2))^{3/2} \text{Im} \left(h_3^H h_2^{H\dagger} \right) \right. \\ &\quad \left. + 2m_Z^2 \left(\sqrt{Q^2(Q^2 - 4m_Z^2)} (2m_Z^2 - Q^2) \text{Im} \left(h_3^H h_1^{H\dagger} \right) + (4m_Z^2 - Q^2) Q^2 \text{Re} \left(h_1^H h_2^{H\dagger} \right) \right) \right) \\ &\quad - s_\phi \left((Q^2(Q^2 - 4m_Z^2))^{3/2} \text{Re} \left(h_2^H h_3^{H\dagger} \right) \right. \\ &\quad \left. + 2m_Z^2 \left(\sqrt{Q^2 - 4m_Z^2} (Q^2 - 2m_Z^2) \text{Re} \left(h_1^H h_3^{H\dagger} \right) + (4m_Z^2 - Q^2) Q^2 \text{Im} \left(h_1^H h_2^{H\dagger} \right) \right) \right) \\ &\quad + 4c_\phi m_Z^4 (2m_Z^2 - 4Q^2) |h_1^H|^2. \end{aligned} \quad (26)$$

Although the terms dependent on the ϕ angle vanish after integration in the phase space, the study of observables related to ϕ can lead to interesting results.

C. $H^* \rightarrow Z(p_1)Z(p_2) \rightarrow \bar{\ell}_1 \ell_1 \bar{\ell}_2 \ell_2$ decay width

Following the discussion of Appendix A, the differential $H^* \rightarrow Z(p_1)Z(p_2) \rightarrow \bar{\ell}_1 \ell_1 \bar{\ell}_2 \ell_2$ decay width can be written as

$$\frac{d\Gamma_{H^* \rightarrow \bar{\ell}_1 \ell_1 \bar{\ell}_2 \ell_2}}{dp_1^2 dp_2^2 d \cos \theta_1 d \cos \theta_2 d\phi} = \frac{\sqrt{Q^2 - 4m_Z^2}}{512(2\pi)^6 Q^2} \mathcal{M}_{H^* \rightarrow \bar{\ell}_1 \ell_1 \bar{\ell}_2 \ell_2}^2. \quad (27)$$

Since we consider the scenario where both Z gauge bosons are on-shell, we use the narrow-width approximation for their Breit-Wigner propagators

$$\lim_{m_Z \Gamma_Z \rightarrow 0} \frac{1}{(p_i^2 - m_Z^2) + (m_Z \Gamma_Z)^2} = \delta(p_i^2 - m_Z^2) \frac{\pi}{m_Z \Gamma_Z}, \quad (i = 1, 2), \quad (28)$$

which allows one to integrate over p_1 and p_2 . Introducing the polarized and interference amplitudes the differential decay width can be written as

$$\frac{d\Gamma_{H^* \rightarrow \bar{\ell}_1 \ell_1 \bar{\ell}_2 \ell_2}}{d \cos \theta_1 d \cos \theta_2 d\phi} = \frac{\sqrt{Q^2 - 4m_Z^2}}{(32\sqrt{2})^2 (2\pi)^4 Q^2 (m_Z \Gamma_Z)^2} \left(\sum_{\lambda} \mathcal{M}_{H^* \rightarrow Z(p_1)Z(p_2)}^2(\lambda, \lambda) \mathcal{M}_{Z(p_1) \rightarrow \bar{\ell}_1 \ell_1}^2(\lambda) \mathcal{M}_{Z(p_2) \rightarrow \bar{\ell}_2 \ell_2}^2(\lambda) + \mathcal{M}_{\text{int}}^2 \right). \quad (29)$$

All our results presented below will be obtained from the above equation along with Eqs. (18)–(22), whereas the interference term (23) will be integrated out as we are mainly interested in the polarization effects.

Below we present the $H^* \rightarrow \bar{\ell}_1 \ell_1 \bar{\ell}_2 \ell_2$ decay width in the scenario with polarized Z gauge bosons, though for completeness we also consider the case of unpolarized Z gauge bosons, which can be obtained via standard calculation techniques and serve to cross-check our results for polarized Z gauge bosons obtained from Eq. (29).

1. Polarized $H^* \rightarrow \bar{\ell}_1 \ell_1 \bar{\ell}_2 \ell_2$ decay width

To obtain the polarized $H^* \rightarrow \bar{\ell}_1 \ell_1 \bar{\ell}_2 \ell_2$ decay width we integrate Eq. (29) over the angular variables in the region given in Appendix A, which after some rearrangement yields

$$\Gamma_{H^* \rightarrow \bar{\ell}_1 \ell_1 \bar{\ell}_2 \ell_2}^{\lambda} = \frac{g^6 (g_A^2 + g_V^2)^2 \sqrt{Q^2 - 4m_Z^2}}{(48\sqrt{2})^2 (2\pi)^3 Q^2 c_W^6 m_Z^4 \Gamma_Z^2} F^{\lambda}(Q^2), \quad (30)$$

with

$$\begin{aligned} F^{\lambda}(Q^2) = & \left((Q^2 - 2m_Z^2)^2 \left(4m_Z^4 |h_1^H|^2 + Q^4 |h_2^H|^2 \right) + 4Q^2 m_Z^2 (Q^4 - 6Q^2 m_Z^2 + 8m_Z^4) \text{Re} \left(h_1^H h_2^{H\dagger} \right) \right) f_0 \\ & + 4m_Z^4 \left(4m_Z^2 \sqrt{Q^2 (Q^2 - 4m_Z^2)} \text{Im} \left(h_3^H h_1^{H\dagger} \right) + Q^2 (Q^2 - 4m_Z^2) |h_3^H|^2 + 4m_Z^4 |h_1^H|^2 \right) f_L \\ & + 4m_Z^2 \left(-4m_Z^2 \sqrt{Q^2 (Q^2 - 4m_Z^2)} \text{Im} \left(h_3^H h_1^{H\dagger} \right) + Q^2 (Q^2 - 4m_Z^2) |h_3^H|^2 + 4m_Z^4 |h_1^H|^2 \right) f_R, \end{aligned} \quad (31)$$

where the f_L , f_R and f_0 coefficients must be set to 0 or 1 according to the polarization λ of the Z gauge bosons. For instance, $f_L = 1$ and $f_R = f_0 = 0$ correspond to $\lambda = L$. As already pointed out, the interference term in Eq. (29) vanishes after ϕ integration. Thus, it is possible to discriminate between the distinct contributions of polarized Z gauge bosons, which are functions of the four-lepton invariant mass only.

The polarized $H^* \rightarrow \bar{\ell}_1 \ell_1 \bar{\ell}_2 \ell_2$ decay width can also be written in terms of the $Z(p_i) \rightarrow \bar{\ell}_i \ell_i$ branching fractions as follows

$$\Gamma_{H^* \rightarrow \bar{\ell}_1 \ell_1 \bar{\ell}_2 \ell_2}^{\lambda} = 2 \Gamma_{H^* \rightarrow ZZ}^{\lambda}(Q^2) \text{Br}(Z \rightarrow \ell_1 \bar{\ell}_1) \text{Br}(Z \rightarrow \ell_2 \bar{\ell}_2) = 0.00226418 \times \Gamma_{H^* \rightarrow Z_{\lambda} Z_{\lambda}}(Q^2), \quad (32)$$

where an extra factor of 2 is included in Eq. (32), which stems from the fact that the Z bosons are not in the final state, and hence we have not considered the statical factor of 1/2 that corrects the double-counting of identical particles in the $H^* \rightarrow ZZ$ amplitude. This factor has been overlooked in the past [6]. In Eq. (32), the polarized $H^* \rightarrow Z_{\lambda} Z_{\lambda}$ decay width is given by

$$\Gamma_{H^* \rightarrow Z_{\lambda} Z_{\lambda}}^{\lambda} = \frac{g^2 \sqrt{Q^2 - 4m_Z^2}}{128\pi Q^2 c_W^2 m_Z^6} F^{\lambda}(Q^2). \quad (33)$$

and we have used

$$\text{Br}(Z \rightarrow \ell_i \bar{\ell}_i) \simeq \frac{g^2 m_Z}{12\pi c_W^2 \Gamma_Z} (g_A^2 + g_V^2) \simeq 0.0336466, \quad (34)$$

in the massless lepton approximation [70].

From (32) it is clear that the four-lepton final state is sensitive to the polarization effects on the HZZ vertex: the polarization of the Z gauge bosons determine the $H^* \rightarrow ZZ \rightarrow \bar{\ell}_1 \ell_1 \bar{\ell}_2 \ell_2$ decay width. Therefore, the left-right asymmetry in Z gauge boson pair production [7] has also effects on the decay of an off-shell Higgs boson into four-leptons. Such an asymmetry is a consequence of CP violation due to complex anomalous couplings. Hence, new physics effects may be detected via transversally polarized Z gauge bosons [71]. Moreover, they would provide an excellent probe of quantum field theory, which predicts that the h_i^V ($i=1, 2, 3$) form factors are complex [56]. On the other hand, longitudinally polarized Z gauge bosons are not useful to detect CP -violating effects, though it is still possible to detect new-physics contributions through the \hat{c}_Z anomalous coupling, which enters into the definition of the h_1^H form factor.

2. Unpolarized $H^* \rightarrow \bar{\ell}_1 \ell_1 \bar{\ell}_2 \ell_2$ decay width

For the sake of completeness, we also consider unpolarized Z gauge bosons. From Eq. (30), we can obtain the unpolarized $H^* \rightarrow \bar{\ell}_1 \ell_1 \bar{\ell}_2 \ell_2$ decay width by setting $f_L = f_R = f_0 = 1$, which yields

$$\Gamma_{H^* \rightarrow \bar{\ell}_1 \ell_1 \bar{\ell}_2 \ell_2}(Q^2) = \frac{g^6 (g_A^2 + g_V^2)^2 \sqrt{Q^2 - 4m_Z^2}}{(48\sqrt{2})^2 (2\pi)^3 Q^2 c_W^6 m_Z^4 \Gamma_Z^2} G(Q^2), \quad (35)$$

where

$$G^\lambda(Q^2) = Q^2 (Q^2 - 4m_Z^2) \left(Q^2 (Q^2 - 4m_Z^2) |h_2^H|^2 + 8m_Z^4 |h_3^H|^2 \right) + 4m_Z^4 (Q^4 - 4Q^2 m_Z^2 + 12m_Z^4) |h_1^H|^2 + 4Q^2 m_Z^2 (Q^4 - 6Q^2 m_Z^2 + 8m_Z^4) \text{Re} \left(h_1^H h_2^H \right). \quad (36)$$

To cross-check this result, we have inserted the left-hand side of Eq. (12) into Eq. (8) and used standard calculation techniques. In this case, the boosts defined in Appendix A are necessary as the square amplitude depends on scalar products of four-momentum given in their respective $Z(p_i)$ gauge boson rest frame.

From Eq. (35) we can observe that the contribution of the CP -violating form factor h_3^H to the four-lepton final state is suppressed as compared to the CP -conserving contributions, which are proportional to higher powers of the four-lepton invariant mass Q . Thus, the $H^* \rightarrow \bar{\ell}_1 \ell_1 \bar{\ell}_2 \ell_2$ unpolarized decay width is not really sensitive to CP -violating effects. We also note that one can extract from Eq. (35) the tree-level SM contribution, which is obtained for $h_2^H = h_3^H = 0$ and $h_1^H = 1$. As far as the one-loop level SM contribution is concerned, it is induced by setting $h_3^H = 0$, whereas the remaining form factors are given in terms of \hat{b}_Z only since \hat{c}_Z vanishes at this order. The one-loop level contribution to \hat{b}_Z was reported in Ref. [7].

Eq. (35) can be written in the following short form

$$\Gamma_{H^* \rightarrow \bar{\ell}_1 \ell_1 \bar{\ell}_2 \ell_2} = 2 \Gamma_{H^* \rightarrow ZZ}(Q^2) \text{Br}(Z \rightarrow \ell_1 \bar{\ell}_1) \text{Br}(Z \rightarrow \ell_2 \bar{\ell}_2) = 0.00226418 \times \Gamma_{H^* \rightarrow ZZ}(Q^2), \quad (37)$$

where the unpolarized $H^* \rightarrow ZZ$ decay width for complex anomalous couplings is given by

$$\Gamma_{H^* \rightarrow ZZ}(Q^2) = \frac{g^2 \sqrt{Q^2 - 4m_Z^2}}{512\pi Q^2 c_W^2 m_Z^6} G(Q^2). \quad (38)$$

The inclusion of a factor of 2 in Eq. 37 has already been explained when obtaining the polarized decay width. The unpolarized $H^* \rightarrow ZZ \rightarrow \bar{\ell}_1 \ell_1 \bar{\ell}_2 \ell_2$ process has been studied long ago. Thus, we can find both theoretical and numerical results in the literature [72–77].

III. NUMERICAL ANALYSIS

We now turn to the study of the polarized $H^* \rightarrow \bar{\ell}_1 \ell_1 \bar{\ell}_2 \ell_2$ decay width and a few observables sensitive to new physics effects. We first present a cross-check of our numerical evaluation method, which relies on the analytical results presented in Sec. II along with the kinematics and four-body phase space discussed in Appendix A.

A. Consistency of our numerical evaluation method

Using our analytical results, we have implemented a Mathematica code to perform a numerical evaluation, which is available in our GitLab repository [78]. For an alternative numerical evaluation, we have implemented the Lagrangian of Eq. (1) into `MadGraph5_aMC@NLO` [79] via the UFO format [80] using the FeynRules package [81]. We then compare the numerical results obtained via these two independent methods. The $e^-e^+\mu^-\mu^+$ final state is considered in our analysis, which, however, is indistinguishable from other $\ell_1\ell_1\bar{\ell}_2\ell_2$ final states as the massless lepton approximation is used.

Since the anomalous HZZ couplings have negligible effects on the unpolarized $H^* \rightarrow \bar{\ell}_1\ell_1\bar{\ell}_2\ell_2$ decay width [7], we set $h_1^H = 1$ and $h_2^H = h_3^H = 0$ and calculate the tree-level SM contribution to the unpolarized $H^* \rightarrow ZZ \rightarrow e^-e^+\mu^-\mu^+$ and $H^* \rightarrow ZZ$ decays. The results obtained by our own numerical evaluation method and `MadGraph5_aMC@NLO` are shown in Fig. 3 as functions of the four-lepton invariant mass. An excellent agreement between both results is observed, with a slight variation of the order of 2 % of the decay widths. We have also verified that the $H^* \rightarrow ZZ \rightarrow e^-e^+\mu^-\mu^+$ decay width obtained via Eq. (37) agree with that obtained from Eq. (35) and shown in the left plot of Fig. 3, which in turn shows the consistency of the extra factor of 2 inserted into Eq. (37). Finally, our numerical results agree with those reported in Ref. [72].

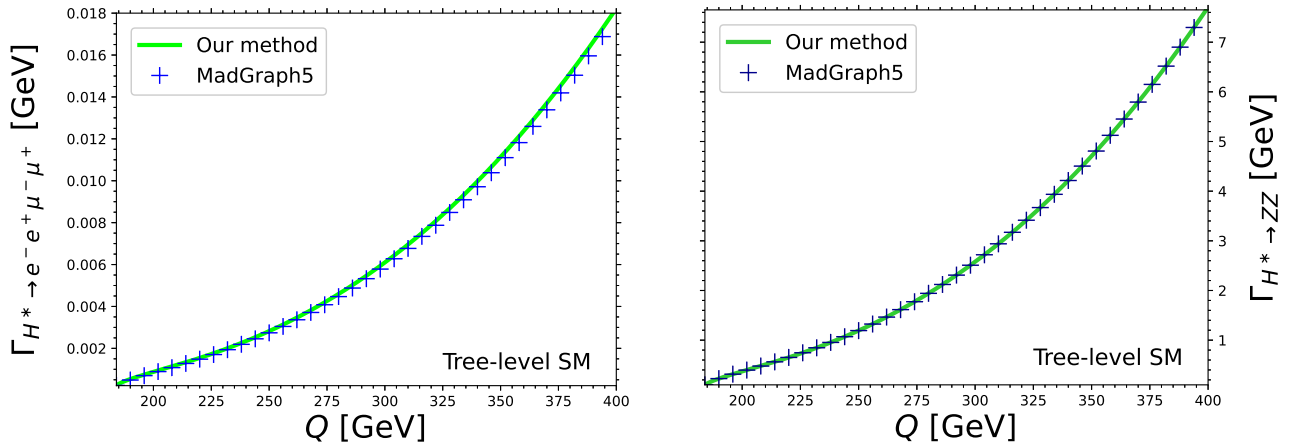


FIG. 3. Tree-level SM contribution to the unpolarized $H^* \rightarrow ZZ \rightarrow e^-e^+\mu^-\mu^+$ and $H^* \rightarrow ZZ$ decay widths as functions of the four-lepton invariant mass Q obtained by both our own evaluation method and `MadGraph5_aMC@NLO`.

We now turn to cross-check the numerical results for the polarized $H^* \rightarrow ZZ$ decay width, which is sensitive to the anomalous HZZ couplings and yields the unpolarized $H^* \rightarrow ZZ \rightarrow e^-e^+\mu^-\mu^+$ decay via Eq. (32). For our numerical evaluation method, we use the analytical result of Eq. (33) for the polarized partial decay widths $\Gamma_{H^* \rightarrow Z_\lambda Z_\lambda}$. We show in the left (right) plots of Fig. 4 the behavior of the $H^* \rightarrow Z_L Z_L$ ($H^* \rightarrow Z_R Z_R$) decay width as a function of the four-lepton invariant mass for two sets of values of the anomalous HZZ couplings consistent with the most stringent bounds [7]. For comparison purposes, we also show the tree-level SM contributions.

Again, we can conclude that the results obtained by our numerical evaluation method and `MadGraph5_aMC@NLO` agree nicely. We observe that the anomalous contributions yield a significant deviation from the tree-level SM contribution for large Q , and also note that the $H^* \rightarrow Z_\lambda Z_\lambda$ decay width shows a distinctive behavior for each polarization in both scenarios of new physics. As discussed below, this stems from the CP -violating effects due to the complex \hat{b}_Z form factor, which have already been studied through a left-right asymmetry in the decay $H^* \rightarrow Z_\lambda Z_\lambda$ [7]. A more detailed analysis of the polarized $H^* \rightarrow \bar{\ell}_1\ell_1\bar{\ell}_2\ell_2$ decay widths, including the SM contribution up to one-loop level, together with the analysis of other interesting observables sensitive to new physics will be presented below.

In summary, there is an excellent agreement between the results obtained by our evaluation method and `MadGraph5_aMC@NLO`. We also corroborate the consistency of Eqs. (37) and (32), which allows one to study the four-lepton decay widths using the $H^* \rightarrow ZZ$ decay width only. Note that in our evaluation method, we consider a constant Γ_Z decay width in the narrow width approximation, whereas in `MadGraph5_aMC@NLO` the complex mass scheme is used. According to Ref. [82], both methods yield the same results for four-leptons in the final state. In the following, we will use our evaluation method as it is more suited for our analysis.

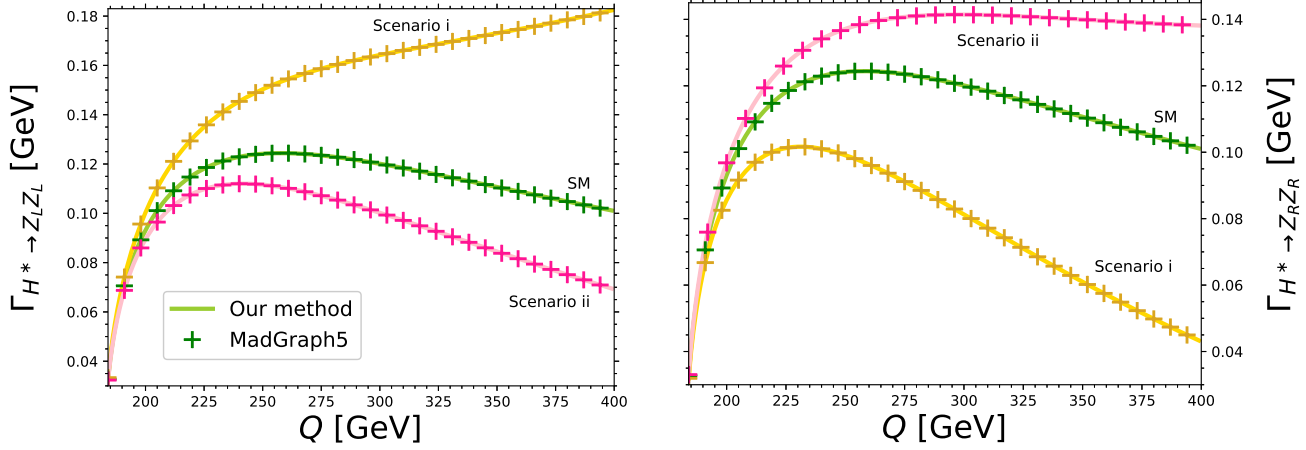


FIG. 4. Behavior of the polarized $H^* \rightarrow Z_L Z_L$ (left plot) and $H^* \rightarrow Z_R Z_R$ (right plot) decay widths as functions of the four-lepton invariant mass for two sets of values of the anomalous couplings: scenario i) $\hat{b}_Z = 0.001 + i0.003$, $\hat{c}_Z = 0.001 + i0.002$, and $\tilde{b}_Z = 0.01 + i0.02$; scenario ii) $\hat{b}_Z = 0.0001 + i0.001$, $\hat{c}_Z = 0.0001 + i0.001$, and $\tilde{b}_Z = 0.001 - i0.01$. We also show the SM tree-level contributions for comparison purposes. For the numerical evaluation we use our own evaluation method and `MadGraph5_aMC@NLO`.

B. Polarized decay widths

The physics of polarizations of weak bosons at the LHC has been discussed in Refs. [50, 58, 59], whereas those related to the Z boson are of particular interest as they are being measured by the CMS, ATLAS and LHCb collaborations [34–38]. To study the polarized Z boson effects, we now consider the most general case with complex HZZ anomalous couplings and examine three realistic scenarios for their numerical values. For the \hat{b}_Z anomalous coupling, we will consider the SM contribution up to the one-loop level. That result has been reported in Ref. [7] in terms of the Passarino-Veltman scalar functions and as a function of Q , the four-lepton invariant mass. The numerical evaluation of \hat{b}_Z is obtained through the `LoopTools` package [83]. While, for the \hat{c}_Z and \tilde{b}_Z anomalous couplings, we use the stringent limits obtained through LHC data and theoretical results [3, 7]. They are shown in Table I. Note that although we consider a non-vanishing \hat{c}_Z , it yields a negligible contribution to the h_1^H form factor, and hence the same values are considered for the three scenarios. Finally, the one-loop SM contribution is also studied to compare with the new physics scenarios.

TABLE I. Scenarios for the HZZ anomalous couplings used in our analysis of the $H^* \rightarrow e^- e^+ \mu^- \mu^+$ decay. For the \hat{b}_Z coupling, we consider SM contribution up to one-loop level [7], whereas for the remaining anomalous couplings, the stringent limits obtained through LHC data and theoretical results are used.

Scenario	\tilde{b}_Z	\hat{c}_Z
1	$0.01 + i0.02$	$0.0001 + 0.0003i$
2	$0.001 - i0.01$	$0.0001 + 0.0003i$
3	$0.0001 + i0.001$	$0.0001 + 0.0003i$

We first analyze the effects of the Z gauge bosons polarizations on the $H^* \rightarrow ZZ \rightarrow e^- e^+ \mu^- \mu^+$ decay, for which we can use either Eq. (30) or Eq. (32) as they yield the same results. We show in Fig. 5 the results for the left- and right-handed polarized $H^* \rightarrow e^- e^+ \mu^- \mu^+$ decay widths as functions of Q . The longitudinally polarized Z gauge bosons are not considered as for this case, the $H^* \rightarrow ZZ \rightarrow e^- e^+ \mu^- \mu^+$ decay width is not sensitive to the CP -violating anomalous coupling \tilde{b}_Z .

We observe in Fig. 5 that for small values of the real and absorptive parts of the CP -violating anomalous coupling \tilde{b}_Z (scenario 3), the polarized $\Gamma_{H^* \rightarrow e^- e^+ \mu^- \mu^+}^\lambda$ decay widths shows a little variation from the pure SM contribution,

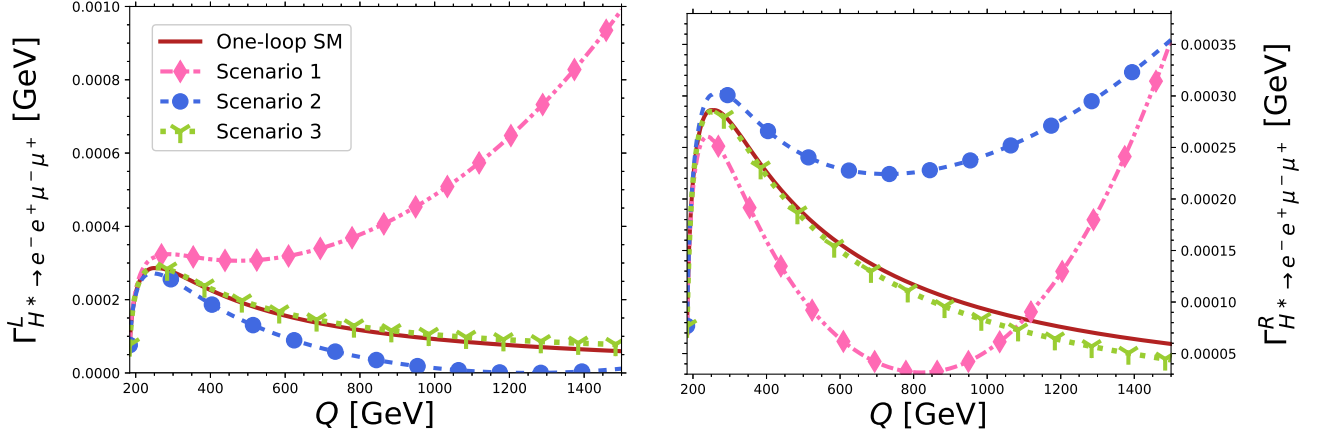


FIG. 5. Behavior of the transversally polarized $\Gamma_{H^* \rightarrow e^- e^+ \mu^- \mu^+}^\lambda$ decay widths ($\lambda = L, R$) for the SM contribution and the three scenarios of Table I for the anomalous HZZ couplings.

though such a deviation increases slightly as Q grows, being more appreciable in the case of right-handed polarization. On the other hand, in scenarios 1 and 2, in which \tilde{b}_Z is assumed to be relatively large, a considerable deviation from the SM contribution develops around $Q = 250$ GeV and becomes larger as Q increases. Therefore, the effects of the complex anomalous HZZ couplings in the four-lepton final state are more notable at high energies. Furthermore, in scenario 1, $\Gamma_{H^* \rightarrow Z_L Z_L}$ is an increasing function of Q and is larger than the tree-level SM contribution, whereas $\Gamma_{H^* \rightarrow Z_R Z_R}$ decreases around $Q = 225$ GeV and is smaller than the tree-level SM contribution. For scenario 2 the contrary is true. Thus, an apposite behavior between the left and right polarized widths is observed.

Finally, in Fig. 5, we note that the partial width increases significantly at high energies for some new physics scenarios, as the non-SM contributions in Eq. (18)-(19) are proportional to powers of Q . A similar behavior has been observed in trilinear neutral gauge bosons couplings [84, 85], where the unitarity can be preserved if we generalize the \tilde{b}_Z and \tilde{c}_Z anomalous couplings as

$$\tilde{c}_Z(Q^2) = \frac{\tilde{c}_{Z0}}{(1 + Q^2/\Lambda^2)^n}, \quad \tilde{b}_Z(Q^2) = \frac{\tilde{b}_{Z0}}{(1 + Q^2/\Lambda^2)^n}, \quad (39)$$

where \tilde{c}_{Z0} and \tilde{b}_{Z0} are constants, which can be determined by considering unitarity conditions of the $gg \rightarrow H^* \rightarrow ZZ$ process [86], whereas the parameter Λ is an energy scale introduced to avoid unphysical results as Q increases. It is noted in Eq. (39) that the $\tilde{c}_Z(Q^2)$ and $\tilde{b}_Z(Q^2)$ anomalous couplings are approximately constants for $Q \ll \Lambda$. Therefore, our results in Fig. 5 are valid for an energy scale $\Lambda \gg 1$ TeV, since we have considered the values in Table I and there is no significant change in the one-loop SM contribution [7]. In general, the parameter Λ is fixed to the order of TeVs or ∞ [70, 84]. For the latter case, the results obtained in this work remain unchanged. Nevertheless, for $\Lambda \sim 1$ TeV the size of our predicted effects will reduce. The values of Λ and n still have to be determined for the HZZ anomalous couplings, but this is beyond the scope of this work

C. Left-right asymmetry \mathcal{A}_{LR}

The behavior of the $H^* \rightarrow e^- e^+ \mu^- \mu^+$ polarized amplitudes give rise to a left-right asymmetry \mathcal{A}_{LR}

$$\mathcal{A}_{LR} = \frac{\Gamma_{H^* \rightarrow e^- e^+ \mu^- \mu^+}^L - \Gamma_{H^* \rightarrow e^- e^+ \mu^- \mu^+}^R}{\Gamma_{H^* \rightarrow e^- e^+ \mu^- \mu^+}^L + \Gamma_{H^* \rightarrow e^- e^+ \mu^- \mu^+}^R}, \quad (40)$$

which is non-vanishing as long as complex anomalous couplings are present and can be written as

$$\mathcal{A}_{LR} = \frac{4m_Z^2 \sqrt{Q^2(Q^2 - 4m_Z^2)} \text{Im} \left(h_3^H h_1^{H\dagger} \right)}{Q^2(Q^2 - 4m_Z^2) |h_3^H|^2 + 4m_Z^4 |h_1^H|^2}, \quad (41)$$

thereby being suitable for detecting CP -violating effects.

In Fig. 6, we show the behavior of \mathcal{A}_{LR} as a function of the four-lepton invariant mass in the three scenarios of Table I for the anomalous HZZ couplings. The SM contribution is not shown since it vanishes at the one-loop level. We observe that for scenario 2, in which the real and absorptive parts of h_3^H are of opposite sign, the \mathcal{A}_{LR} magnitude can be larger than for the other cases. Also, it is noted that in the three scenarios, \mathcal{A}_{LR} reaches its largest magnitude at a relatively high Q , and hence the CP -violating effects would be more significant beyond the $2m_Z$ threshold. Nevertheless, the asymmetry tends to decrease as Q grows, which stems from the fact that it behaves as a $1/Q^2$ function at high energies.

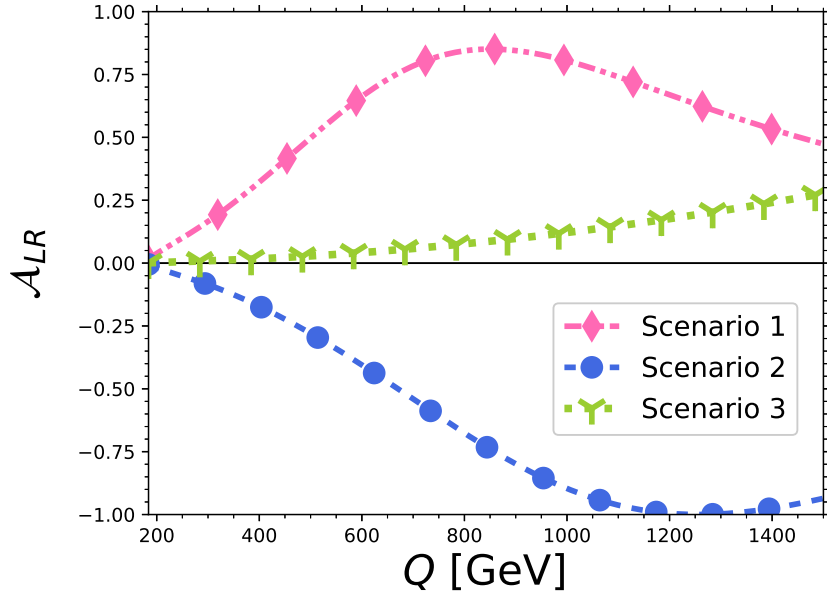


FIG. 6. Left-right asymmetry \mathcal{A}_{LR} as a function of the four-lepton invariant mass in the three scenarios of Table I for the anomalous HZZ couplings.

The results of Figs. 5 and 6, together with Eq. (41), are in agreement with those reported in Ref. [7] for the $H^* \rightarrow Z_\lambda Z_\lambda$ process, which is a consequence of the four-leptons final state being a function of Q and independent of the $Z \rightarrow \ell\ell$ processes (see Eq. 32). On the other hand, the angular variables only appear in the production of lepton pairs and could also serve to detect any new physics effects from the HZZ anomalous couplings.

D. Angular distributions

The Higgs decay to four lepton is the cleanest channel to access to the polarizations of the weak bosons, as they can be studied through the angular observables of the leptons produced by the Z bosons decays [50, 59]. For that reason, we now turn to analyze the role of the angular variables in the polarized $H^* \rightarrow e^- e^+ \mu^- \mu^+$ decay widths. These angular distributions together with the Z bosons polarizations are being measured at the LHC [36–39, 51]. As we pointed out, the results obtained in this work remain unchanged for an energy scale $\Lambda \gg 1$ TeV. Usually values for Λ of this order are considered to set limits on similar anomalous couplings to those considered in the HZZ interaction [70]. Since the angle ϕ only enters into the interference term of the full square amplitude, its effects are unobservable through polarized Z gauge bosons. After the integration of Eq. (29) over ϕ , the differential $H^* \rightarrow e^- e^+ \mu^- \mu^+$ decay width will be in terms of the angles $\theta_{1,2}$. Therefore, it is still possible to study the polarization effects in the four lepton-final state through the angular variables. From Eq. (21) we observe that the left- and right-handed square amplitudes are symmetric in both θ_1 and θ_2 angles, which is evident in Fig. 7, where we show the contours of the SM contribution to the transversally polarized $H^* \rightarrow e^- e^+ \mu^- \mu^+$ differential decay widths in the c_{θ_1} vs c_{θ_2} plane for $Q = 500$ GeV. The left-handed polarized case reaches its higher values around $\cos \theta_i = -1$, whereas for the right polarization this occurs at $\cos \theta_i = 1$. In these regions the partial widths can be of order 10^{-4} . Future experimental

searches should focus on these specific angular regions to increase the sensitivity to potential deviations from the SM predictions. The smallest values are obtained around $\cos \theta_i \approx 0$ in both scenarios. Furthermore, it is found that the transversely polarized differential decay widths for $H^* \rightarrow e^- e^+ \mu^- \mu^+$ exhibit similar behavior for other values of Q and when non-zero anomalous couplings are considered.

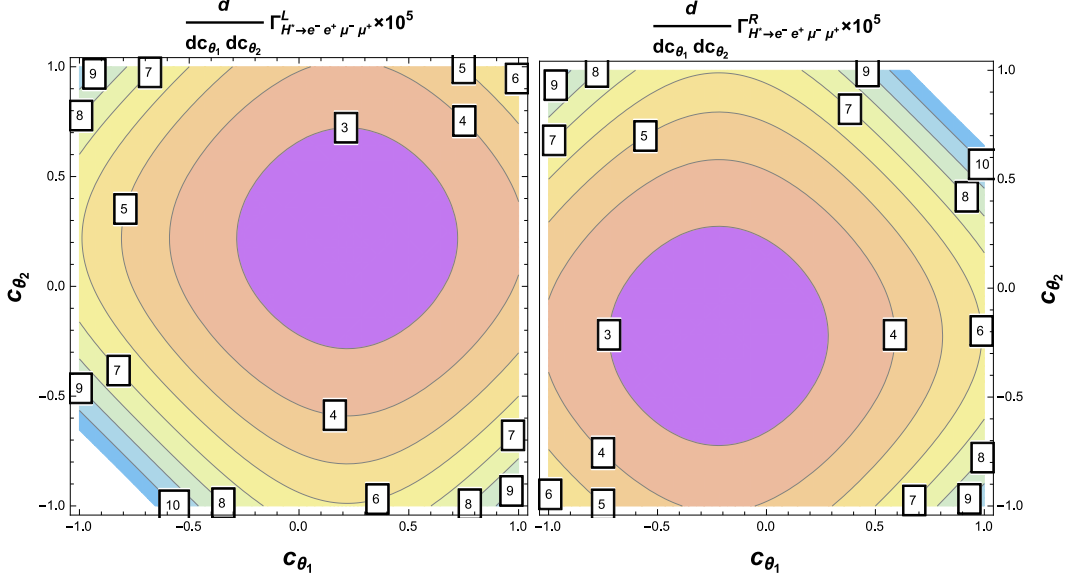


FIG. 7. Contours of the transversely polarized $H^* \rightarrow e^- e^+ \mu^- \mu^+$ differential decay widths in the c_{θ_1} vs c_{θ_2} plane for $Q = 500$ GeV. We only include the SM one-loop contribution.

We now consider the three scenarios of Table I for the anomalous HZZ couplings and study their effects on the polarized $H^* \rightarrow e^- e^+ \mu^- \mu^+$ angular distributions after integrating over ϕ and one of the angles $\theta_{1,2}$. The results are presented in Figs. 8 and 9 as functions of the cosine of the remaining angle c_{θ_i} . It is observed that the angular distributions show a significant deviation from the SM contribution in scenarios 1 and 2, which becomes more pronounced at large Q . However, in scenario 3, where small values for the real and absorptive parts of the anomalous h_3^H coupling are considered, the deviation is insignificant for small Q , though it becomes noticeable as Q becomes large, particularly in the case of right-handed polarization. We also note that, for left-handed polarization, the differential decay width is always above (below) the SM contribution in scenario 1 (scenario 2), whereas the opposite is true for right-handed polarization. Also, the left-handed (right-handed) polarized angular distributions reach their larger magnitude as $c_{\theta_i} \rightarrow -1$ ($c_{\theta_i} \rightarrow 1$). This distinctive behavior of the angular distributions for each transverse polarization of the Z gauge bosons stems from the fact that the terms that give rise to the left-right asymmetry \mathcal{A}_{LR} of Eq. (41) and the terms proportional to c_{θ_i} in Eq. (21), which have opposite signs, remain unchanged after ϕ integration. This hints at new asymmetries associated with the angular variables, which we will analyze below. We also would like to point out that the results shown in Figs. 8 and 9 for the SM contributions agree with those reported in Ref. [58]. Some technics to identify Z bosons polarizations through angular variables at the LHC have been addressed in Refs. [13, 59, 87], whereas using polarized beams in the future ILC or different $e^+ e^-$ colliders have been also studied in Refs. [22, 88, 89]. These approaches may be extended to observe the polarized angular distributions at high-energy colliders.

1. Polarized asymmetries

As some asymmetries from the HZZ coupling can be large enough to give evidence of new physics at the LHC [15] and motivated by the behavior of the $H^* \rightarrow e^- e^+ \mu^- \mu^+$ angular distributions for transverse polarizations, we define the following angular left-right asymmetry

$$\mathcal{A}_{LR\theta} = \frac{\frac{d}{dc_{\theta_i}} \Gamma_{H^* \rightarrow e^- e^+ \mu^- \mu^+}^L - \frac{d}{dc_{\theta_i}} \Gamma_{H^* \rightarrow e^- e^+ \mu^- \mu^+}^R}{\frac{d}{dc_{\theta_i}} \Gamma_{H^* \rightarrow e^- e^+ \mu^- \mu^+}^L + \frac{d}{dc_{\theta_i}} \Gamma_{H^* \rightarrow e^- e^+ \mu^- \mu^+}^R}, \quad (42)$$

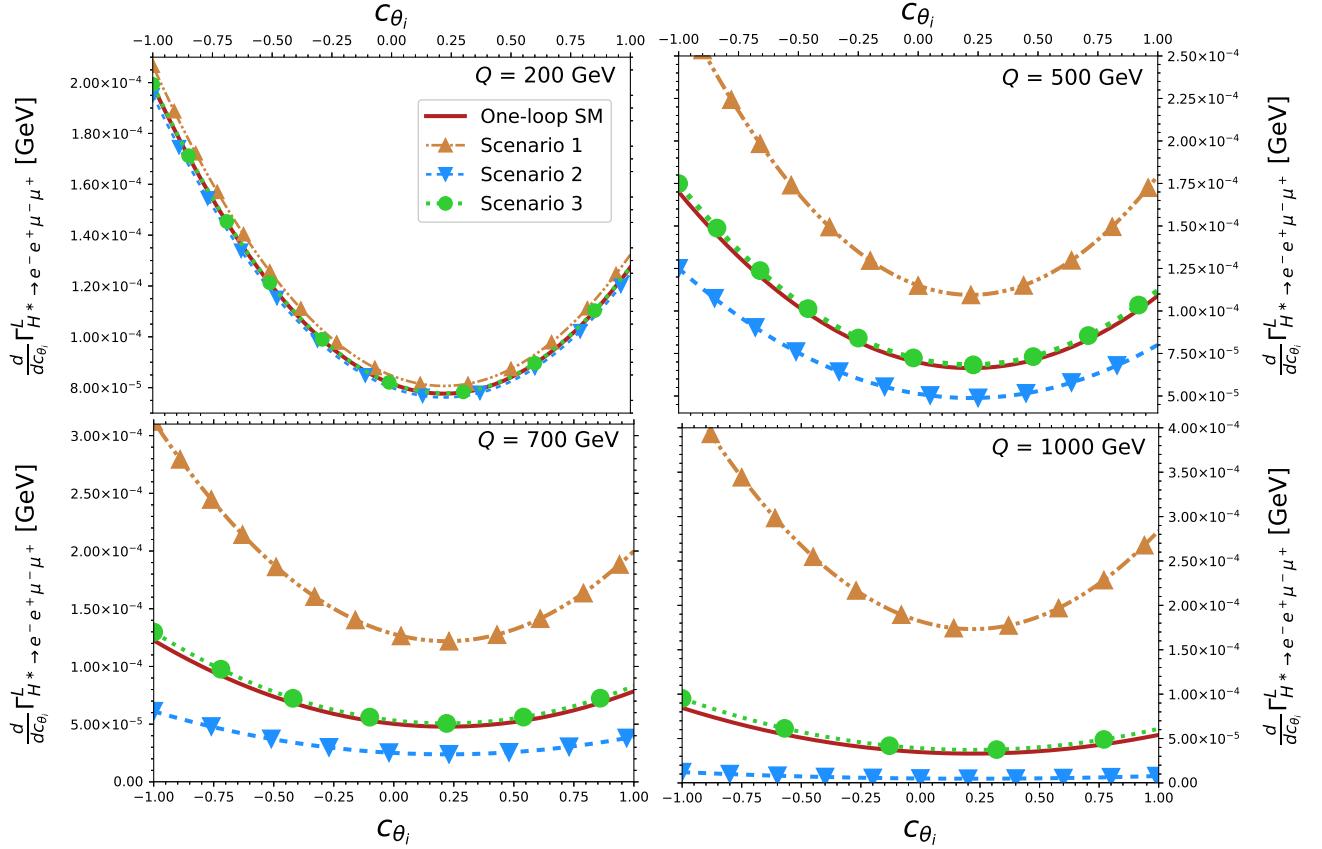


FIG. 8. Differential $H^* \rightarrow e^- e^+ \mu^- \mu^+$ decay width for left-handed polarization as a function of $\cos \theta_i$ ($i = 1, 2$) for a few values of the four-lepton invariant mass Q in the three scenarios of Table I for the anomalous HZZ couplings. The SM contribution up to the one-loop level is included. We already integrated over one of the two angles.

where $i = 1$ (2) and the angle θ_2 (θ_1) was integrated over. Since $\Gamma_{H^* \rightarrow e^- e^+ \mu^- \mu^+}$ is symmetric under θ_i ($i = 1, 2$), the same expression holds for both angles. The analytical form, obtained through Eq. (29), can be written as

$$\mathcal{A}_{LR\theta} = -\frac{4}{m_Z^2} \frac{f(Q^2, c_{\theta_i})}{h(Q^2, c_{\theta_i})}, \quad (43)$$

with the $f(Q^2, c_{\theta_i})$ and $h(Q^2, c_{\theta_i})$ functions given as

$$\begin{aligned} f(Q^2, c_{\theta_i}) = & g_A g_V c_{\theta_i} m_Z^2 \left(Q^2 (Q^2 - 4m_Z^2) |h_3^H|^2 + 4m_Z^4 |h_1^H|^2 \right) \\ & - (g_A^2 + g_V^2) (1 + c_{\theta_i}^2) \left(m_Z^4 \sqrt{Q^2 (Q^2 - 4m_Z^2)} \text{Im} (h_3^H h_1^{H\dagger}) \right), \end{aligned} \quad (44)$$

$$\begin{aligned} h(Q^2, c_{\theta_i}) = & -16 g_A g_V c_{\theta_i} m_Z^2 \sqrt{Q^2 (Q^2 - 4m_Z^2)} \text{Im} (h_3^H h_1^{H\dagger}) \\ & + (g_A^2 + g_V^2) (1 + c_{\theta_i}^2) \left(Q^2 (Q^2 - 4m_Z^2) |h_3^H|^2 + 4m_Z^4 |h_1^H|^2 \right), \end{aligned} \quad (45)$$

where the terms proportional to $g_{V,A}^2$ in $f(Q^2, c_{\theta_i})$ are identical to those in the \mathcal{A}_{LR} asymmetry Eq. (41), whereas the remaining terms arise from those proportional to c_{θ_i} in the $H^* \rightarrow e^- e^+ \mu^- \mu^+$ amplitude, which have been not integrated out yet. Furthermore, it is noted that if the numerator and denominator Eq. (43) are integrated over c_{θ_i} we obtain the non-angular \mathcal{A}_{LR} asymmetry. Although the \mathcal{A}_{LR} and $\mathcal{A}_{LR\theta}$ asymmetries are related, they have

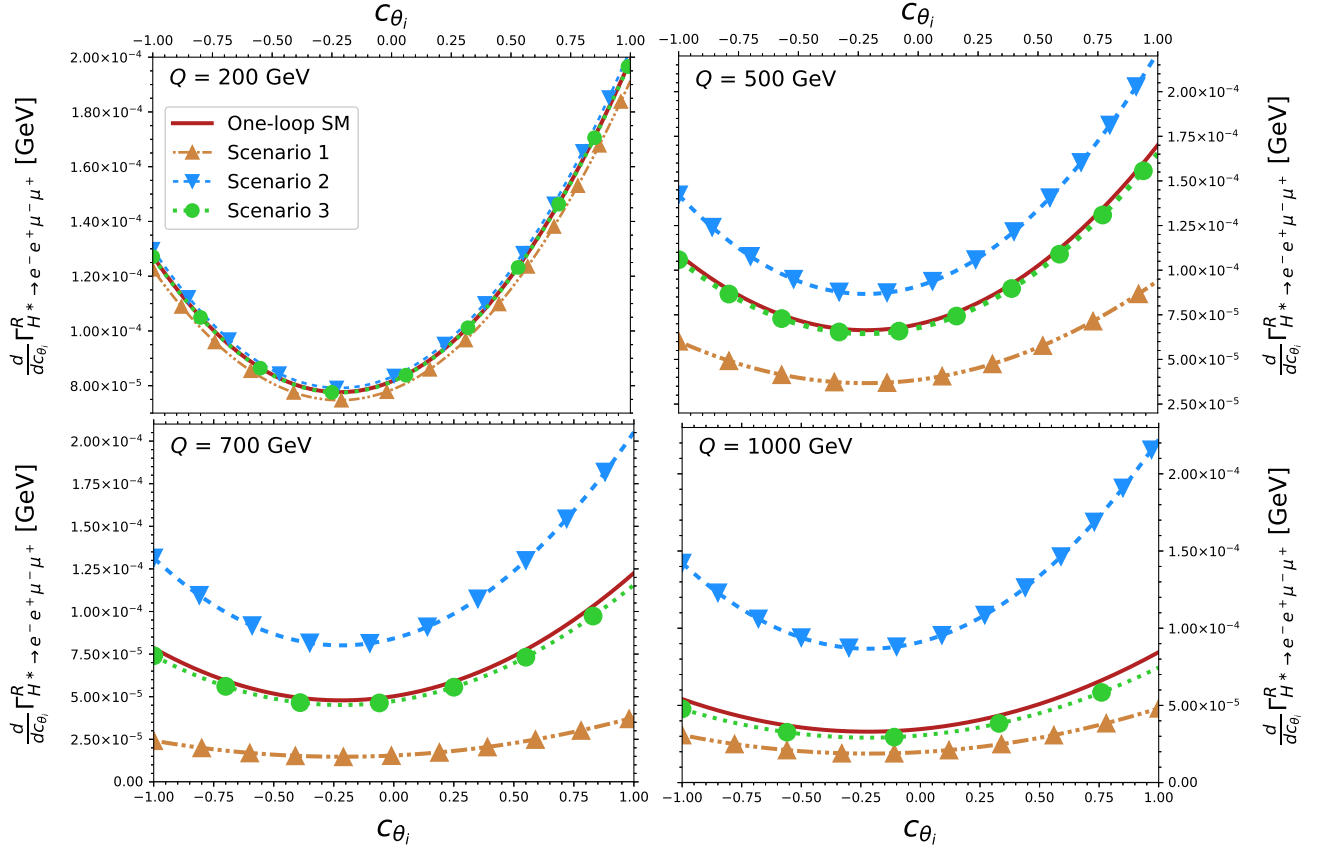


FIG. 9. The same as in Fig. 8, but for right-handed polarizations.

a distinct origin: the former is induced via the HZZ anomalous couplings, and the latter is a result of polarized Z gauge bosons decaying into leptons, where the angular variables appear. It is also worth noting that even for a vanishing CP -violating form factor h_3^H , the $\mathcal{A}_{LR\theta}$ asymmetry is non-zero, thereby being non-vanishing in the SM at the one-loop level:

$$\mathcal{A}_{LR\theta}^{\text{SM}} = -\frac{4g_A g_V c_{\theta_i}}{(g_A^2 + g_V^2)(1 + c_{\theta_i}^2)}. \quad (46)$$

Again we consider the three scenarios of Table I for the anomalous HZZ couplings and evaluate the effects on the $\mathcal{A}_{LR\theta}$ asymmetry. The results are shown in Fig. 10, where the SM contribution is also included. We observe that at low Q , $\mathcal{A}_{LR\theta}$ shows a slight deviation from the SM in scenarios 1 and 2, which becomes more significant as Q increases, whereas such a variation is negligible in scenario 3. It is interesting to note that the deviation of $\mathcal{A}_{LR\theta}$ from the SM value is of the order of $10^{-1} - 10^{-2}$, whereas the corresponding difference of the polarized $H^* \rightarrow e^- e^+ \mu^- \mu^+$ decay widths concerning the SM contribution is of the order of $10^{-4} - 10^{-5}$. Thus, there may be more possibilities to observe the effects of CP violation through the $\mathcal{A}_{LR\theta}$ asymmetry than in the polarized differential widths.

Given the behavior observed in the polarized differential $H^* \rightarrow e^- e^+ \mu^- \mu^+$ decay width, we also expect the presence of a polarized forward-backward asymmetry, which in general can be defined as follows for the polarized $H^* \rightarrow \bar{f}_i f_i \bar{f}_j f_j$ decay

$$\mathcal{A}_{FB}^\lambda = \frac{\int_0^1 dc_{\theta_i} \frac{d}{dc_{\theta_i}} \Gamma_{H^* \rightarrow \bar{f}_i f_i \bar{f}_j f_j}^\lambda - \int_{-1}^0 dc_{\theta_i} \frac{d}{dc_{\theta_i}} \Gamma_{H^* \rightarrow \bar{f}_i f_i \bar{f}_j f_j}^\lambda}{\int_0^1 dc_{\theta_i} \frac{d}{dc_{\theta_i}} \Gamma_{H^* \rightarrow \bar{f}_i f_i \bar{f}_j f_j}^\lambda + \int_{-1}^0 dc_{\theta_i} \frac{d}{dc_{\theta_i}} \Gamma_{H^* \rightarrow \bar{f}_i f_i \bar{f}_j f_j}^\lambda}. \quad (47)$$

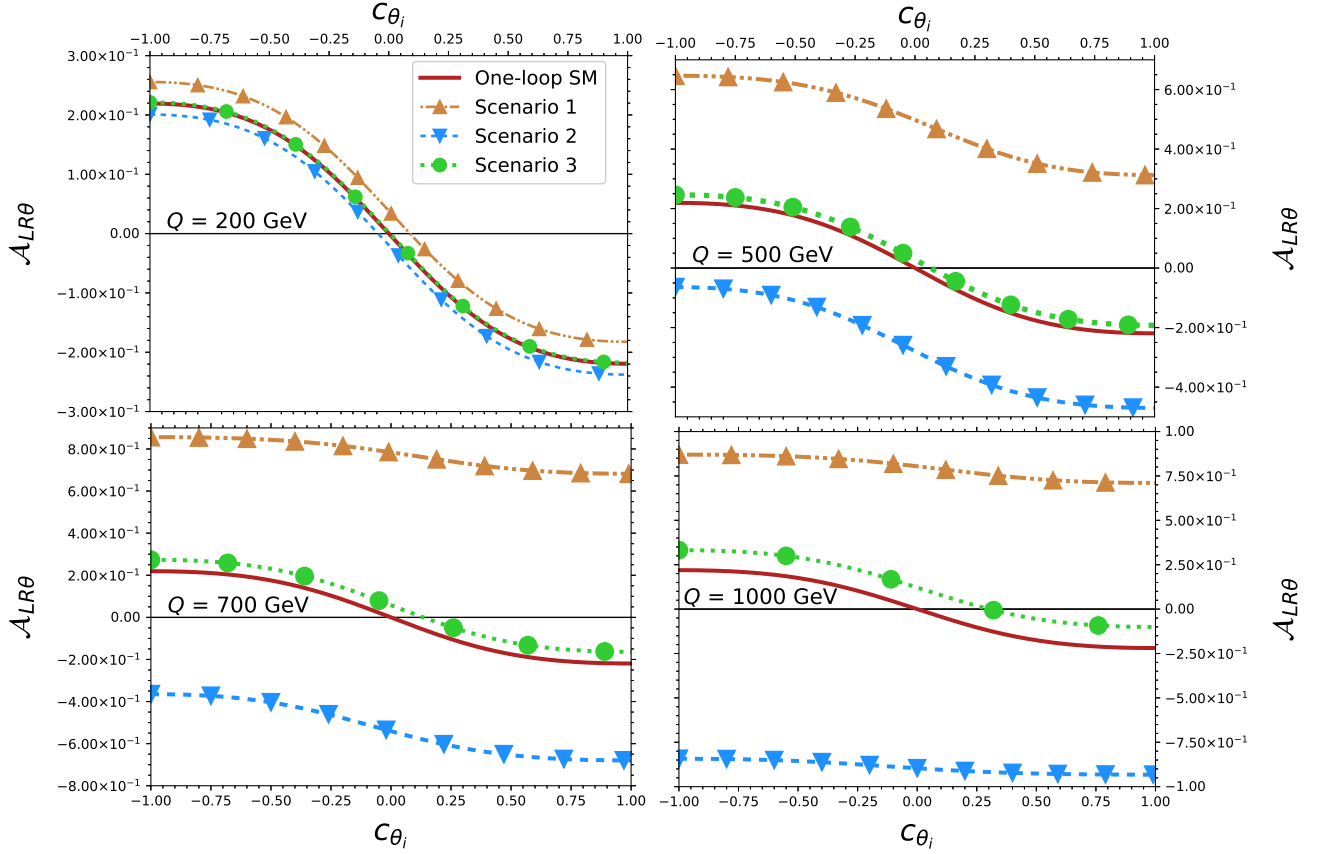


FIG. 10. Behavior of the left-right asymmetry $\mathcal{A}_{LR\theta}$ as a function $\cos \theta_i$ for a few values of the four-lepton invariant mass Q in the three scenarios of Table I for the anomalous HZZ couplings. We also include the SM contribution up to the one-loop level.

A straightforward calculation yields

$$\mathcal{A}_{FB}^{L/R} = \mp \frac{3g_A g_V}{2(g_A^2 + g_V^2)}. \quad (48)$$

Such a simple expression stems from the fact that $\mathcal{A}_{FB}^{L/R}$ is due to the $Z \rightarrow \bar{\ell}\ell$ decay, thereby being independent the anomalous HZZ couplings and the four-lepton invariant mass: it is constant even in new-physics scenarios but a difference of sign arises for left-handed and right-handed polarizations.

We present in Table II the values of the \mathcal{A}_{FB}^λ asymmetry for all the combinations of light fermion flavors in the $H^* \rightarrow \bar{f}_i f_i \bar{f}_j f_j$ final state. We consider massless fermions and distinct fermion-antifermion pairs. It is also noted that the result of Eq. (48) is similar to the left-right Z gauge boson asymmetry in the SM [90, 91].

TABLE II. $\mathcal{A}_{FB}^{L/R}$ asymmetry for all combinations of distinct pairs of light fermion-antifermion flavors in the $H^* \rightarrow \bar{f}_i f_i \bar{f}_j f_j$ decay. The fermion masses have been neglected.

f_i	f_j	$\mathcal{A}_{FB}^{L/R}$
e, μ, τ	e, μ, τ	∓ 0.164
ν_e, ν_μ, ν_τ	ν_e, ν_μ, ν_τ	∓ 0.75
d, s, b	d, s, b	∓ 0.705
u, c	u, c	∓ 0.524

2. Unpolarized asymmetries

Up to now, we have focused only on the effects of the Z gauge boson polarizations in the $H^* \rightarrow ZZ \rightarrow \bar{\ell}_1 \ell_1 \bar{\ell}_2 \ell_2$ decay. Nevertheless, the change of sign in Eq. (48) hints the presence of a forward-backward asymmetry \mathcal{A}_{FB} in the unpolarized case, which is defined as follows

$$\mathcal{A}_{FB} = \frac{\int_0^1 dc_{\theta_i} \frac{d}{dc_{\theta_i}} \Gamma_{H^* \rightarrow ZZ \rightarrow e^- e^+ \mu^- \mu^+} - \int_{-1}^0 dc_{\theta_i} \frac{d}{dc_{\theta_i}} \Gamma_{H^* \rightarrow ZZ \rightarrow e^- e^+ \mu^- \mu^+}}{\int_0^1 dc_{\theta_i} \frac{d}{dc_{\theta_i}} \Gamma_{H^* \rightarrow ZZ \rightarrow e^- e^+ \mu^- \mu^+} + \int_{-1}^0 dc_{\theta_i} \frac{d}{dc_{\theta_i}} \Gamma_{H^* \rightarrow ZZ \rightarrow e^- e^+ \mu^- \mu^+}}. \quad (49)$$

After inserting Eq. (29) we obtain

$$\mathcal{A}_{FB} = -\frac{48 g_A g_V m_Z^6 Q \sqrt{Q^2 - 4m_Z^2}}{(g_A^2 + g_V^2)} \frac{\text{Im} \left(h_3^H h_1^{H\dagger} \right)}{G(Q^2)}, \quad (50)$$

where the $G(Q^2)$ function was given in (36). We note that \mathcal{A}_{FB} vanishes in the SM at the one-loop level since $h_3^H = 0$. Our result reproduces the one reported in Ref. [15], where the absorptive part of h_1^H was dismissed. However, such a term is induced at the one-loop level in the SM, and its contribution provided that a non-vanishing new-physics contribution to h_3^H is present, could be larger than that arising from the corresponding real part [7]. Thus, our result is more complete than those previously reported in the literature.

In contrast with the polarized forward-backward asymmetry, which is due only to the $Z \rightarrow \bar{\ell}_i \ell_i$ decay, the unpolarized one depends on the properties of both the $H^* \rightarrow ZZ$ and the $Z \rightarrow \bar{\ell}_i \ell_i$ decays: the dependence on the complex anomalous couplings is a reflect of the former and the presence of the vector g_V and axial g_A couplings arises from the latter.

We show in Fig. 11 the unpolarized forward-backward asymmetry \mathcal{A}_{FB} as a function of the four-lepton invariant mass in the three scenarios of Table I for the anomalous HZZ couplings. In addition to the anomalous contributions, we have included the one-loop SM contribution to the real and absorptive parts of the h_1^H form factor. Similar to the above results for other observables, \mathcal{A}_{FB} can reach the largest values in scenarios 1 and 2, being of the order of 10^{-3} at most, whereas it is one order of magnitude below in scenario 3. While \mathcal{A}_{FB} can be large at small energies, it tends to vanish at very large Q . An opposite behavior is observed for the \mathcal{A}_{LR} and $\mathcal{A}_{LR\theta}$ asymmetries, which can reach values two orders of magnitude larger than that of \mathcal{A}_{FB} . To our knowledge, the \mathcal{A}_{FB} asymmetry has not been analyzed in the literature.

3. ϕ distributions

The effects of the anomalous couplings on ϕ distributions have been neglected up this point as they have been integrated out in previous sections. These effects can be studied through the interference term $\mathcal{M}_{\text{int}}^2$ (Eq. (23)) after integrating Eq. (29) over c_{θ_i} ($i=1, 2$). In Fig. 12, we show the numerical results of the $H^* \rightarrow e^- e^+ \mu^- \mu^+$ partial width as a function of the azimuthal angle ϕ for the SM at one-loop level and the three scenarios in Table I for the HZZ anomalous couplings. It is observed that larger values of $\Gamma_{H^* \rightarrow e^- e^+ \mu^- \mu^+}$ are obtained at high energies, where the new physics effects are also notable as significant deviations from the SM are found. Furthermore, a shift between

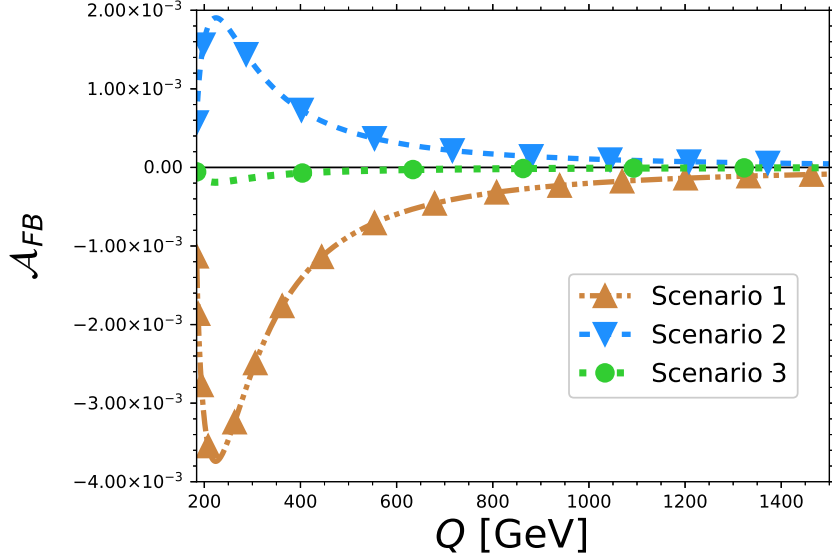


FIG. 11. Behavior of the unpolarized forward-backward asymmetry \mathcal{A}_{FB} as a function of the four-lepton invariant mass Q in the three scenarios of Table I for the anomalous HZZ couplings. The one-loop SM contribution to the h_1^H form factor has been added to the new-physics contribution.

the cases with non-SM anomalous couplings and the SM case is also observed. The consequences of the anomalous couplings are more pronounced for Scenario 1, which considers the largest values of the CP -violating form factor.

The shift observed in the ϕ distributions leads to the definition of the \mathcal{A}_ϕ azimuthal asymmetry

$$\mathcal{A}_\phi = \frac{\int_{\pi}^{2\pi} d\phi \frac{d}{d\phi} \Gamma_{H^* \rightarrow ZZ \rightarrow e^- e^+ \mu^- \mu^+} - \int_0^\pi d\phi \frac{d}{d\phi} \Gamma_{H^* \rightarrow ZZ \rightarrow e^- e^+ \mu^- \mu^+}}{\int_{\pi}^{2\pi} d\phi \frac{d}{d\phi} \Gamma_{H^* \rightarrow ZZ \rightarrow e^- e^+ \mu^- \mu^+} + \int_0^\pi d\phi \frac{d}{d\phi} \Gamma_{H^* \rightarrow ZZ \rightarrow e^- e^+ \mu^- \mu^+}}. \quad (51)$$

After integrating Eq. (29) we obtain

$$\mathcal{A}_\phi = -\frac{9 \pi g_A^2 g_V^2 m_Z^2 Q \sqrt{Q^2 - 4m_Z^2}}{2(g_A^2 + g_V^2)^2} \frac{K(Q^2)}{G(Q^2)}, \quad (52)$$

with

$$K(Q^2) = -2m_Z^2 Q^2 \left[\text{Re} \left(h_1^H h_3^{H\dagger} \right) - 2\text{Re} \left(h_2^H h_3^{H\dagger} \right) \right] + 4m_Z^4 \text{Re} \left(h_1^H h_3^{H\dagger} \right) - Q^4 \text{Re} \left(h_2^H h_3^{H\dagger} \right), \quad (53)$$

and the $G(Q^2)$ function defined in Eq. (36). From Eq. (53), it is clear that the \mathcal{A}_ϕ asymmetry is very sensitive to the CP -violating form factor h_3^H . We show in Fig. 13 the \mathcal{A}_ϕ asymmetry as a function of the four-lepton invariant mass for the three new physics scenarios, whereas the SM case is not considered as it is zero. Once again, the largest values are reached for Scenario 1, which are order 10^{-4} . For scenario 3, we obtain smaller results, since they are of order 10^{-6} . Contrary to the behavior observed for the \mathcal{A}_{FB} asymmetry, we find that the \mathcal{A}_ϕ does not vanish at $Q > 1000$ GeV. Thus, the azimuthal asymmetry may be measured at super high energies.

The ϕ distributions are also good channels for observing the effects of anomalous couplings. Our SM results are in agreement with those reported in Ref. [15], nonetheless, the anomalous couplings contributions are very different, as the shift was not observed, and therefore the azimuthal asymmetry has not been studied in the form presented in this work.

In brief, the azimuthal distributions are sensitive to new physics, particularly to CP -violating effects. They can provide deeper insights into the potential impact on observables at high-energy colliders.

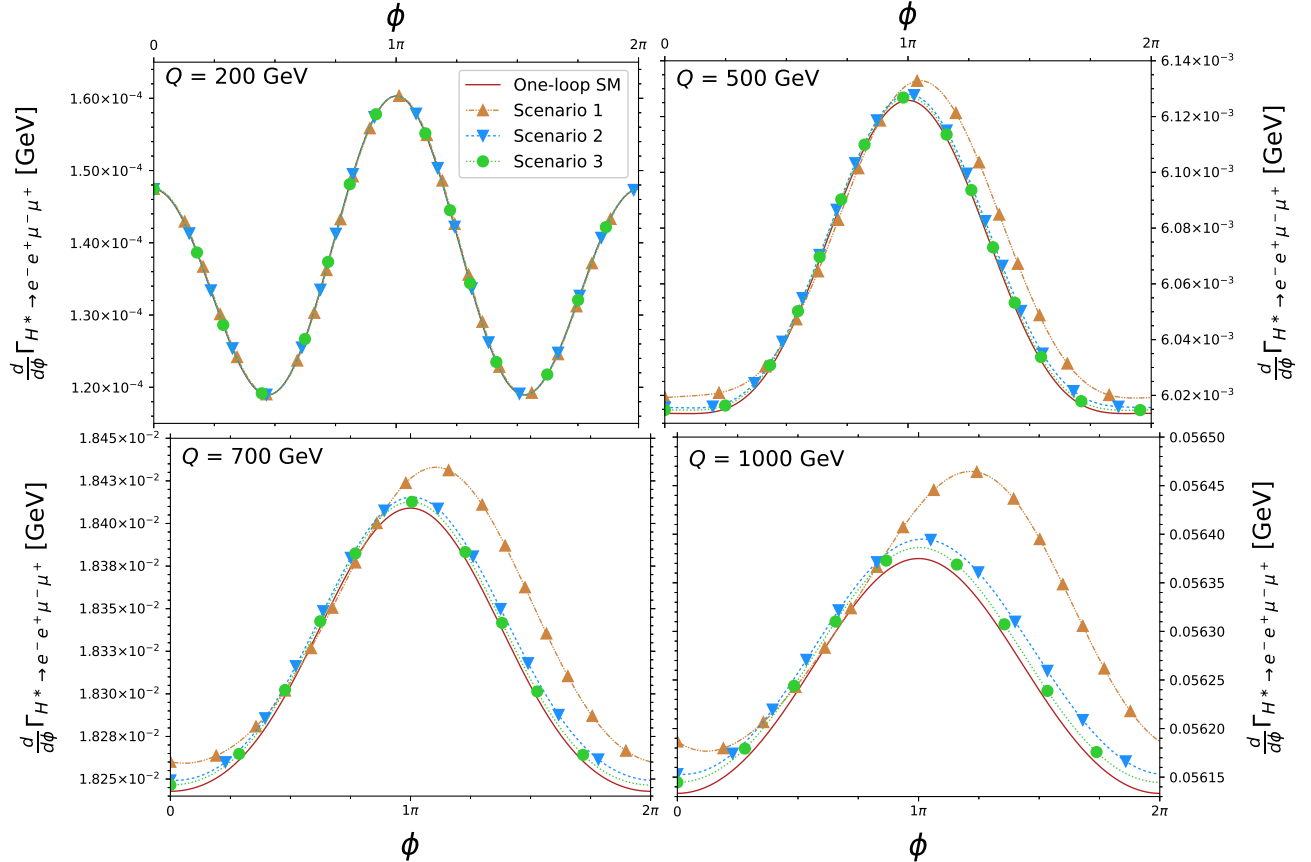


FIG. 12. Differential $H^* \rightarrow e^- e^+ \mu^- \mu^+$ decay width as a function of ϕ for various values of the four-lepton invariant mass Q in the three scenarios of Table I for the anomalous HZZ couplings. The SM contribution up to the one-loop level is included.

IV. CONCLUSIONS AND OUTLOOK

We have presented a novel analysis of the $H^* \rightarrow ZZ \rightarrow \bar{\ell}_1 \ell_1 \bar{\ell}_2 \ell_2$ decay width for both unpolarized and polarized Z gauge bosons considering the most general H^*ZZ vertex function, which is parametrized by three form factors h_i^H ($i=1, 2, 3$), where the SM contributions up to the one-loop level and anomalous contributions arising from new-physics are included. We then consider the scenario where all the h_i^H couplings are complex, which to our knowledge has never been studied in the literature, and obtain analytical results for both the unpolarized and polarized $H^* \rightarrow ZZ \rightarrow \bar{\ell}_1 \ell_1 \bar{\ell}_2 \ell_2$ square amplitudes, out of which the decay widths, angular distributions, and left-right (forward-backward) asymmetries can be straightforwardly obtained. Our results reproduce previous ones obtained in more restrictive scenarios. It is found that the polarized $H^* \rightarrow ZZ \rightarrow \bar{\ell}_1 \ell_1 \bar{\ell}_2 \ell_2$ decay is mainly determined by the $H^* \rightarrow ZZ$ one for the four-lepton invariant mass distributions.

To cross-check the consistency of our numerical evaluation method we use `MadGraph5_aMC@NLO`, with the corresponding Feynman rules for our model obtained via the `FeynRules` package. For the numerical analysis we consider some realistic scenarios for the complex HZZ anomalous couplings, consistent with the current experimental and indirect constraints, and analyze the role of the transversal (left-handed and right-handed) polarizations of the Z gauge bosons on the behavior of the $H^* \rightarrow ZZ \rightarrow \bar{\ell}_1 \ell_1 \bar{\ell}_2 \ell_2$ decay width as a function of the four-lepton invariant mass Q , which turns out to be very distinctive for each type of longitudinal polarization. We found that for some specific values of the complex HZZ couplings, the polarized $H^* \rightarrow ZZ \rightarrow \bar{\ell}_1 \ell_1 \bar{\ell}_2 \ell_2$ decay width can deviate considerably from the SM contribution, but such a deviation is more pronounced at large Q . An opposite behavior between the left and right-handed polarizations is observed. This leads to a left-right asymmetry \mathcal{A}_{LR} , which vanishes in the SM as requires the presence of CP -violating anomalous couplings. The angular distributions of the $H^* \rightarrow ZZ \rightarrow \bar{\ell}_1 \ell_1 \bar{\ell}_2 \ell_2$ decay are also analyzed, which exhibits similar behavior to that observed for the invariant mass distributions. Hence,

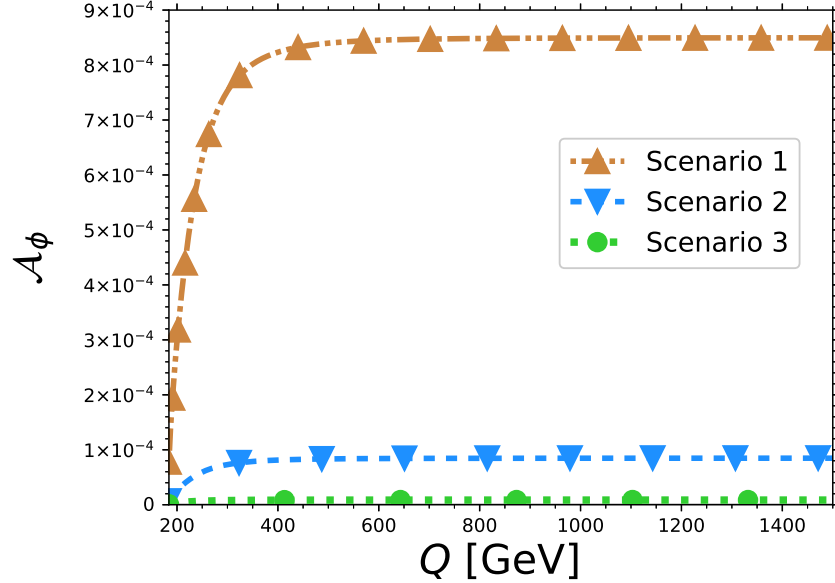


FIG. 13. Behavior of the azimuthal asymmetry \mathcal{A}_ϕ as a function of the four-lepton invariant mass Q in the three scenarios of Table I for the anomalous HZZ couplings. The one-loop SM contribution to the h_1^H form factor has been added to the new-physics contribution.

we introduce an angular left-right asymmetry $\mathcal{A}_{LR\theta}$ that has a non-vanishing SM one-loop level contribution but shows considerable deviations due to complex anomalous HZZ couplings. Finally, a polarized forward-backward asymmetry \mathcal{A}_{FB}^λ is studied, which is found to be constant but differs by a sign for left-handed and right-handed polarizations of the Z gauge bosons. It is also worth noting that the $H^* \rightarrow ZZ \rightarrow \bar{\ell}_1 \ell_1 \bar{\ell}_2 \ell_2$ decay is unsusceptible to new-physics effects in the case of longitudinally polarized Z gauge bosons. For completeness, we also study the scenario with unpolarized Z gauge bosons, where the forward-backward \mathcal{A}_{FB}^λ and azimuthal \mathcal{A}_ϕ asymmetries as a function of the four-lepton invariant mass are examined, where a different behavior compared with the \mathcal{A}_{LR} asymmetry is found.

In summary, the study of the off-shell $H^* \rightarrow ZZ \rightarrow \bar{\ell}_1 \ell_1 \bar{\ell}_2 \ell_2$ decay, via the transverse polarizations of the Z gauge bosons, could be a useful tool to search for effects of new physics due to the real and absorptive parts of the HZZ anomalous couplings, which could lead to significant deviations from the SM contributions in the decay widths as well as other observables such as angular distributions and left-right (forward-backward, azimuthal) asymmetries. In particular, we have put special emphasis on the study of the effects of the absorptive parts of the HZZ anomalous couplings as they have been largely overlooked in the past but can serve as a probe of the SM at the LHC and future colliders. Such absorptive parts are an unique prediction of quantum field theory.

ACKNOWLEDGMENTS

This work was supported by UNAM Posdoctoral Program (POSDOC). We also acknowledge support from Sistema Nacional de Investigadores (Mexico).

Appendix A: Kinematics and phase space for the $H \rightarrow ZZ \rightarrow \bar{\ell}_1 \ell_1 \bar{\ell}_2 \ell_2$ decay

The phase space of an n -body decay was studied by Cabibbo and Maksymowicz [92], Pais and Treiman [93], and Byckling and Kajanate [94–98]. In particular, the $1 \rightarrow 4$ decay can be decomposed through a recursion relation into 3 partial $1 \rightarrow 2$ decays as follows [92, 96, 99]: $1 \rightarrow 2 \rightarrow 1 \rightarrow 2 + 1 \rightarrow 2$. Following this approach we obtain below the differential phase space for the $H \rightarrow ZZ \rightarrow \bar{\ell}_1 \ell_1 \bar{\ell}_2 \ell_2$ decay.

For the four-momenta we use the nomenclature defined in Fig. 1, namely, $H(q) \rightarrow Z(p_1) + Z(p_2)$, followed by $Z(p_1) \rightarrow \ell_1(q_1) + \bar{\ell}_1(q_2)$ and $Z(p_2) \rightarrow \ell_2(q_3) + \bar{\ell}_2(q_4)$. For our calculation we consider the reference systems shown in

Fig. 2. The differential decay width is thus given in terms of the following three angles θ_1 , θ_2 and ϕ angles:

- θ_1 is the angle between \vec{p}_1 and \vec{q}_1 in the rest frame of the $Z(p_1)$ gauge boson.
- θ_2 is the angle between \vec{p}_2 and \vec{q}_3 in the rest frame of the $Z(p_2)$ gauge boson.
- ϕ is the relative angle between the $Z(p_1) \rightarrow 2\ell_1$ and $Z(p_2) \rightarrow 2\ell_2$ decay planes, taken as positive from the $Z(p_1)$ plane to the $Z(p_2)$ plane, with $\phi = 0$ in the case in which both planes coincide and both \vec{q}_1 and \vec{q}_3 are in the same direction.

We now discuss the kinematics for the distinct reference frames introduced above.

1. Off-shell Higgs boson rest frame

The kinematics of the $H^* \rightarrow ZZ$ decay in the Higgs boson rest frame can be described by the following relations

$$q^\mu = (Q, 0), \quad (A1)$$

$$p_{1,2}^\mu = (Q/2, \pm \vec{p}), \quad (A2)$$

where the magnitude of the three-momentum \vec{p} is

$$\|\vec{p}\| = \frac{\sqrt{Q^2 - 4m_Z^2}}{2}. \quad (A3)$$

We consider that in this frame the Z gauge bosons move along the x axis, so their polarization vectors can be written as

$$\epsilon_{1,2}^\mu(0) = \frac{1}{m_Z} \left(\|\vec{p}\|, \pm \frac{\sqrt{Q^2}}{2}, 0, 0 \right), \quad (A4)$$

$$\epsilon_1^\mu(R/L) = \frac{1}{\sqrt{2}} (0, 0, -i, \pm 1). \quad (A5)$$

2. $Z(p_i)$ gauge boson rest frame

In our calculation, we also use the rest frame of a $Z(p_i)$ gauge boson decaying into a lepton-antilepton pair, which obeys the following kinematics

$$p_i^\mu = (m_Z, 0), \quad (A6)$$

$$q_1^\mu = (m_Z/2, \vec{k}_1), \quad q_2^\mu = (m_Z/2, -\vec{k}_1), \quad (A7)$$

$$q_3^\mu = (m_Z/2, \vec{k}_2), \quad q_4^\mu = (m_Z/2, -\vec{k}_2), \quad (A8)$$

where, according to Fig. 2, the three-momenta \vec{k}_i are given as

$$\vec{k}_1 = \frac{\sqrt{m_Z^2 - 4m_{\ell_i}^2}}{2} (\cos \theta_1, \sin \theta_1, 0), \quad (A9)$$

$$\vec{k}_2 = \frac{\sqrt{m_Z^2 - 4m_{\ell_i}^2}}{2} (-\cos \theta_2, \sin \theta_2 \cos \phi, \sin \theta_2 \sin \phi), \quad (A10)$$

whereas the form of the transverse polarization vectors of Eq. (A5) still holds, whereas for longitudinal polarizations we have

$$\epsilon_{1,2}^\mu(0) = (0, \pm 1, 0, 0). \quad (A11)$$

Since the interference term of the $H \rightarrow ZZ \rightarrow \bar{\ell}_1 \ell_1 \bar{\ell}_2 \ell_2$ square amplitude has to be calculated in the Higgs boson frame, we need to boost the four-momenta and polarization vectors defined in the $Z(p_i)$ rest frames into the Higgs boson rest frame, which is achieved via the following Lorentz matrix

$$\Lambda_\nu^\mu = \begin{pmatrix} \gamma & \gamma v & 0 & 0 \\ \gamma v & \gamma & 0 & 0 \\ 0 & 0 & 1 & 0 \\ 0 & 0 & 0 & 1 \end{pmatrix}, \quad (\text{A12})$$

with

$$v = \frac{\vec{p}_i}{E_i} = \pm \frac{\sqrt{Q^2 - 4m_Z^2}}{Q}. \quad (\text{A13})$$

3. Phase space

The $H \rightarrow ZZ \rightarrow \bar{\ell}_1 \ell_1 \bar{\ell}_2 \ell_2$ phase space $d(R_4)$ can be written as

$$d(R_4) = \frac{d^3 q_1}{(2\pi)^3 2E_{q_1}} \frac{d^3 q_2}{(2\pi)^3 2E_{q_2}} \frac{d^3 q_3}{(2\pi)^3 2E_{q_3}} \frac{d^3 q_4}{(2\pi)^3 2E_{q_4}} (2\pi)^4 \delta^4(q - q_1 - q_2 - q_3 - q_4), \quad (\text{A14})$$

where the lepton energies are $E_{q_i} = \sqrt{m_i^2 - \vec{p}_i^2}$ ($i = 1, 2, 3, 4$). We will follow the approach of Ref. [99], which is analogous to that used in [92]. We thus introduce the relations

$$\int \frac{d^3 p_1}{2E_{p_1}} dS_1 \delta^4(p_1 - q_1 - q_2) = 1, \quad (\text{A15})$$

and

$$\int \frac{d^3 p_2}{2E_{p_2}} dS_2 \delta^4(p_2 - q_3 - q_4) = 1, \quad (\text{A16})$$

where $E_{p_i} = \sqrt{\vec{p}_i^2 + S_i}$, with $S_i = p_i^2$ ($i = 1, 2$).

The $d(R_4)$ phase space can thus be written as

$$d(R_4) = \frac{dS_1 dS_2}{(2\pi)^8} I_{p_1} I_{p_2} I_q, \quad (\text{A17})$$

where, in the rest frames of the Z gauge bosons and the Higgs boson, the I_{p_i} and I_q integrals are given for massless leptons as follows

$$I_{p_1} = \int \frac{d^3 q_1}{2E_{q_1}} \frac{d^3 q_2}{2E_{q_2}} \delta^4(p_1 - q_1 - q_2) \quad (\text{A18})$$

$$= \frac{\pi}{4} d \cos \theta_1, \quad (\text{A19})$$

$$I_{p_2} = \int \frac{d^3 q_3}{2E_{q_3}} \frac{d^3 q_4}{2E_{q_4}} \delta^4(p_2 - q_3 - q_4) \quad (\text{A20})$$

$$= \frac{1}{8} d \cos \theta_2 d\phi, \quad (\text{A21})$$

and

$$I_q = \int \frac{d^3 p_1}{2E_{p_1}} \frac{d^3 p_2}{2E_{p_2}} \delta^4(q - p_1 - p_2) \quad (\text{A22})$$

$$= \frac{\pi}{2Q} \sqrt{Q^2 - 4m_Z^2}. \quad (\text{A23})$$

Therefore the $d(R_4)$ phase space reads

$$d(R_4) = \frac{\sqrt{Q^2 - 4m_Z^2}}{256Q(2\pi)^6} dS_1 dS_2 d \cos \theta_1 d \cos \theta_2 d\phi, \quad (\text{A24})$$

For massless leptons, the integration region reads

$$0 < S_2 < \left(Q - \sqrt{S_1} \right)^2, \quad (\text{A25})$$

$$0 < S_1 < Q^2, \quad (\text{A26})$$

$$0 < \theta_1, \theta_2 < \pi, \quad (\text{A27})$$

$$0 < \phi < 2\pi, \quad (\text{A28})$$

where $Q^2 = q^2$ is the invariant mass of the four final leptons, which is the same in all frames of reference and is usually used in LHC analyses. For the purpose of our calculation we denote $Q = \|q\|$.

[1] S. Chatrchyan *et al.* (CMS), Observation of a New Boson at a Mass of 125 GeV with the CMS Experiment at the LHC, *Phys. Lett. B* **716**, 30 (2012), arXiv:1207.7235 [hep-ex].

[2] G. Aad *et al.* (ATLAS), Observation of a new particle in the search for the Standard Model Higgs boson with the ATLAS detector at the LHC, *Phys. Lett. B* **716**, 1 (2012), arXiv:1207.7214 [hep-ex].

[3] A. Tumasyan *et al.* (CMS), Measurement of the Higgs boson width and evidence of its off-shell contributions to ZZ production, *Nature Phys.* **18**, 1329 (2022), arXiv:2202.06923 [hep-ex].

[4] G. Aad *et al.* (ATLAS), Evidence of off-shell Higgs boson production from ZZ leptonic decay channels and constraints on its total width with the ATLAS detector, *Phys. Lett. B* **846**, 138223 (2023), arXiv:2304.01532 [hep-ex].

[5] B. A. Kniehl, Radiative corrections for $H \rightarrow ZZ$ in the standard model, *Nucl. Phys. B* **352**, 1 (1991).

[6] K. H. Phan, D. T. Tran, and A. T. Nguyen, One-loop off-shell decay $H^* \rightarrow ZZ$ at future colliders, (2022), arXiv:2209.12410 [hep-ph].

[7] A. I. Hernández-Juárez, G. Tavares-Velasco, and A. Fernández-Téllez, New evaluation of the HZZ coupling: Direct bounds on anomalous contributions and CP-violating effects via a new asymmetry, *Phys. Rev. D* **107**, 115031 (2023), arXiv:2301.13127 [hep-ph].

[8] A. Soni and R. M. Xu, Probing CP violation via Higgs decays to four leptons, *Phys. Rev. D* **48**, 5259 (1993), arXiv:hep-ph/9301225.

[9] K. Hagiwara, S. Ishihara, J. Kamoshita, and B. A. Kniehl, Prospects of measuring general Higgs couplings at e+ e- linear colliders, *Eur. Phys. J. C* **14**, 457 (2000), arXiv:hep-ph/0002043.

[10] S. S. Biswal, R. M. Godbole, R. K. Singh, and D. Choudhury, Signatures of anomalous VVH interactions at a linear collider, *Phys. Rev. D* **73**, 035001 (2006), [Erratum: *Phys. Rev. D* 74, 039904 (2006)], arXiv:hep-ph/0509070.

[11] S. Dutta, K. Hagiwara, and Y. Matsumoto, Measuring the Higgs-Vector boson Couplings at Linear e^+e^- Collider, *Phys. Rev. D* **78**, 115016 (2008), arXiv:0808.0477 [hep-ph].

[12] M. Javurkova, R. Ruiz, R. C. L. de Sá, and J. Sandesara, Polarized ZZ pairs in gluon fusion and vector boson fusion at the LHC, (2024), arXiv:2401.17365 [hep-ph].

[13] K. Rao, S. D. Rindani, and P. Sarmah, Study of anomalous gauge-Higgs couplings using Z boson polarization at LHC, *Nucl. Phys. B* **964**, 115317 (2021), arXiv:2009.00980 [hep-ph].

[14] B. A. Kniehl, Theoretical aspects of standard model Higgs boson physics at a future e+ e- linear collider, *Int. J. Mod. Phys. A* **17**, 1457 (2002), arXiv:hep-ph/0112023.

[15] R. M. Godbole, D. J. Miller, and M. M. Muhlleitner, Aspects of CP violation in the H ZZ coupling at the LHC, *JHEP* **12**, 031, arXiv:0708.0458 [hep-ph].

[16] K. Rao, S. D. Rindani, P. Sarmah, and B. Singh, Polarized Z cross sections in Higgsstrahlung for the determination of anomalous ZZH couplings, *Phys. Lett. B* **840**, 137847 (2023), arXiv:2304.11573 [hep-ph].

[17] M. Fabbrichesi, R. Floreanini, E. Gabrielli, and L. Marzola, Stringent bounds on HWW and HZZ anomalous couplings with quantum tomography at the LHC, *JHEP* **09**, 195, arXiv:2304.02403 [hep-ph].

[18] I. T. Cakir, O. Cakir, A. Senol, and A. T. Tasci, Probing Anomalous HZZ Couplings at the LHeC, *Mod. Phys. Lett. A* **28**, 1350142 (2013), arXiv:1304.3616 [hep-ph].

[19] B. Şahin, Search for the anomalous ZZH couplings at the CLIC, *Mod. Phys. Lett. A* **34**, 1950299 (2019).

[20] R. Gauld, U. Haisch, and L. Schnell, SMEFT at NNLO+PS: Vh production, *JHEP* **01**, 192, arXiv:2311.06107 [hep-ph].

[21] S. Y. Klein, SusHi 2.0 - Higgs production cross sections in BSM models, *PoS EPS-HEP2023*, 416 (2024), arXiv:2311.05939 [hep-ph].

[22] K. Rao, S. D. Rindani, P. Sarmah, and B. Singh, Z polarization at an e^+e^- collider and properties of decay-lepton angular asymmetries, (2023), arXiv:2311.13473 [hep-ph].

[23] H. Xiong, H. Hou, Z. Qian, Q. Xu, and B. Wang, Electroweak corrections to Higgs boson production via Z Z fusion at the future LHeC, (2023), arXiv:2311.14912 [hep-ph].

[24] K. Asteriadis, S. Dawson, P. P. Giardino, and R. Szafron, Prospects for New Discoveries Through Precision Measurements at e^+e^- Colliders, (2024), arXiv:2406.03557 [hep-ph].

[25] A. M. Sirunyan *et al.* (CMS), Constraints on anomalous Higgs boson couplings using production and decay information in the four-lepton final state, *Phys. Lett. B* **775**, 1 (2017), arXiv:1707.00541 [hep-ex].

[26] A. M. Sirunyan *et al.* (CMS), Measurements of the Higgs boson width and anomalous HVV couplings from on-shell and off-shell production in the four-lepton final state, *Phys. Rev. D* **99**, 112003 (2019), arXiv:1901.00174 [hep-ex].

[27] A. M. Sirunyan *et al.* (CMS), Constraints on anomalous Higgs boson couplings to vector bosons and fermions in its production and decay using the four-lepton final state, *Phys. Rev. D* **104**, 052004 (2021), arXiv:2104.12152 [hep-ex].

[28] G. J. Gounaris, J. Layssac, and F. M. Renard, New and standard physics contributions to anomalous Z and gamma selfcouplings, *Phys. Rev. D* **62**, 073013 (2000), arXiv:hep-ph/0003143.

[29] D. Choudhury, S. Dutta, S. Rakshit, and S. Rindani, Trilinear neutral gauge boson couplings, *Int. J. Mod. Phys. A* **16**, 4891 (2001), arXiv:hep-ph/0011205.

[30] A. I. Hernández-Juárez, A. Moyotl, and G. Tavares-Velasco, Contributions to ZZV^* ($V = \gamma, Z, Z'$) couplings from CP violating flavor changing couplings, *Eur. Phys. J. C* **81**, 304 (2021), arXiv:2102.02197 [hep-ph].

[31] A. I. Hernández-Juárez, G. Tavares-Velasco, and R. Gaitán, Non-diagonal contributions to $Z\gamma V^*$ vertex, polarizations and bounds on $Z\bar{t}q$ couplings, (2022), arXiv:2203.16819 [hep-ph].

[32] A. I. Hernández-Juárez, A. Moyotl, and G. Tavares-Velasco, New estimate of the chromomagnetic dipole moment of quarks in the standard model, *Eur. Phys. J. Plus* **136**, 262 (2021), arXiv:2009.11955 [hep-ph].

[33] A. I. Hernández-Juárez, G. Tavares-Velasco, and A. Moyotl, Chromomagnetic and chromoelectric dipole moments of quarks in the reduced 331 model, *Chin. Phys. C* **45**, 113101 (2021), arXiv:2012.09883 [hep-ph].

[34] G. Aad *et al.* (ATLAS), Evidence of pair production of longitudinally polarised vector bosons and study of CP properties in $ZZ \rightarrow 4\ell$ events with the ATLAS detector at $\sqrt{s} = 13$ TeV, *JHEP* **12**, 107, arXiv:2310.04350 [hep-ex].

[35] G. Aad *et al.* (ATLAS), Observation of gauge boson joint-polarisation states in $W\pm Z$ production from pp collisions at $s=13$ TeV with the ATLAS detector, *Phys. Lett. B* **843**, 137895 (2023), arXiv:2211.09435 [hep-ex].

[36] V. Khachatryan *et al.* (CMS), Angular coefficients of Z bosons produced in pp collisions at $\sqrt{s} = 8$ TeV and decaying to $\mu^+\mu^-$ as a function of transverse momentum and rapidity, *Phys. Lett. B* **750**, 154 (2015), arXiv:1504.03512 [hep-ex].

[37] G. Aad *et al.* (ATLAS), Measurement of the angular coefficients in Z -boson events using electron and muon pairs from data taken at $\sqrt{s} = 8$ TeV with the ATLAS detector, *JHEP* **08**, 159, arXiv:1606.00689 [hep-ex].

[38] R. Aaij *et al.* (LHCb), First Measurement of the $Z \rightarrow \mu^+\mu^-$ Angular Coefficients in the Forward Region of pp Collisions at $s=13$ TeV, *Phys. Rev. Lett.* **129**, 091801 (2022), arXiv:2203.01602 [hep-ex].

[39] G. Aad *et al.* (ATLAS), A precise measurement of the Z -boson double-differential transverse momentum and rapidity distributions in the full phase space of the decay leptons with the ATLAS experiment at $\sqrt{s} = 8$ TeV, *Eur. Phys. J. C* **84**, 315 (2024), arXiv:2309.09318 [hep-ex].

[40] M. Aaboud *et al.* (ATLAS), Measurement of $W^\pm Z$ production cross sections and gauge boson polarisation in pp collisions at $\sqrt{s} = 13$ TeV with the ATLAS detector, *Eur. Phys. J. C* **79**, 535 (2019), arXiv:1902.05759 [hep-ex].

[41] S. Chatrchyan *et al.* (CMS), Measurement of the Polarization of W Bosons with Large Transverse Momenta in $W+J$ Events at the LHC, *Phys. Rev. Lett.* **107**, 021802 (2011), arXiv:1104.3829 [hep-ex].

[42] G. Aad *et al.* (ATLAS), Measurement of the polarisation of W bosons produced with large transverse momentum in pp collisions at $\sqrt{s} = 7$ TeV with the ATLAS experiment, *Eur. Phys. J. C* **72**, 2001 (2012), arXiv:1203.2165 [hep-ex].

[43] M. Aaboud *et al.* (ATLAS), Measurement of the W boson polarisation in $t\bar{t}$ events from pp collisions at $\sqrt{s} = 8$ TeV in the lepton + jets channel with ATLAS, *Eur. Phys. J. C* **77**, 264 (2017), [Erratum: Eur.Phys.J.C 79, 19 (2019)], arXiv:1612.02577 [hep-ex].

[44] V. Khachatryan *et al.* (CMS), Measurement of the W boson helicity fractions in the decays of top quark pairs to lepton + jets final states produced in pp collisions at $\sqrt{s} = 8$ TeV, *Phys. Lett. B* **762**, 512 (2016), arXiv:1605.09047 [hep-ex].

[45] G. Aad *et al.* (CMS, ATLAS), Combination of the W boson polarization measurements in top quark decays using ATLAS and CMS data at $\sqrt{s} = 8$ TeV, *JHEP* **08** (08), 051, arXiv:2005.03799 [hep-ex].

[46] G. Aad *et al.* (ATLAS), Measurement of the polarisation of W bosons produced in top-quark decays using dilepton events at $s=13$ TeV with the ATLAS experiment, *Phys. Lett. B* **843**, 137829 (2023), arXiv:2209.14903 [hep-ex].

[47] A. M. Sirunyan *et al.* (CMS), Measurements of production cross sections of polarized same-sign W boson pairs in association with two jets in proton-proton collisions at $\sqrt{s} = 13$ TeV, *Phys. Lett. B* **812**, 136018 (2021), arXiv:2009.09429 [hep-ex].

[48] D. Buarque Franzosi, O. Mattelaer, R. Ruiz, and S. Shil, Automated predictions from polarized matrix elements, *JHEP* **04**, 082, arXiv:1912.01725 [hep-ph].

[49] M. Hoppe, M. Schönherr, and F. Siegert, Polarised cross sections for vector boson production with SHERPA, (2023), arXiv:2310.14803 [hep-ph].

[50] A. Ballestrero, E. Maina, and G. Pelliccioli, Polarized vector boson scattering in the fully leptonic WZ and ZZ channels at the LHC, *JHEP* **09**, 087, arXiv:1907.04722 [hep-ph].

[51] Vector Boson Scattering prospective studies in the ZZ fully leptonic decay channel for the High-Luminosity and High-Energy LHC upgrades, (2018).

[52] S. Kanemura, M. Kikuchi, K. Sakurai, and K. Yagyu, Gauge invariant one-loop corrections to Higgs boson couplings in non-minimal Higgs models, *Phys. Rev. D* **96**, 035014 (2017), arXiv:1705.05399 [hep-ph].

[53] M. Aoki, S. Kanemura, M. Kikuchi, and K. Yagyu, Radiative corrections to the Higgs boson couplings in the triplet model, *Phys. Rev. D* **87**, 015012 (2013), arXiv:1211.6029 [hep-ph].

[54] C. Englert, Y. Soreq, and M. Spannowsky, Off-Shell Higgs Coupling Measurements in BSM scenarios, *JHEP* **05**, 145, arXiv:1410.5440 [hep-ph].

[55] A. I. Hernández-Juárez, R. Gaitán, and R. Martínez, The $H \rightarrow Z\gamma$ decay and CP violation, (2024), arXiv:2405.03094 [hep-ph].

[56] A. I. Hernández-Juárez, A. Moyotl, and G. Tavares-Velasco, Bounds on the absorptive parts of the chromomagnetic and chromoelectric dipole moments of the top quark from LHC data, *Eur. Phys. J. Plus* **137**, 925 (2022), arXiv:2109.09978 [hep-ph].

[57] K. Hagiwara, R. D. Peccei, D. Zeppenfeld, and K. Hikasa, Probing the Weak Boson Sector in $e^+ e^- \rightarrow W^+ W^-$, *Nucl. Phys. B* **282**, 253 (1987).

[58] E. Maina, Vector boson polarizations in the decay of the Standard Model Higgs, *Phys. Lett. B* **818**, 136360 (2021), arXiv:2007.12080 [hep-ph].

[59] E. Maina and G. Pelliccioli, Polarized Z bosons from the decay of a Higgs boson produced in association with two jets at the LHC, *Eur. Phys. J. C* **81**, 989 (2021), arXiv:2105.07972 [hep-ph].

[60] G. Buchalla, O. Cata, and G. D'Ambrosio, Nonstandard Higgs couplings from angular distributions in $h \rightarrow Z\ell^+\ell^-$, *Eur. Phys. J. C* **74**, 2798 (2014), arXiv:1310.2574 [hep-ph].

[61] S. Berge, S. Groote, J. G. Körner, and L. Kaldmäe, Lepton-mass effects in the decays $H \rightarrow ZZ^* \rightarrow \ell^+\ell^-\tau^+\tau^-$ and $H \rightarrow WW^* \rightarrow \ell\nu\tau\nu\tau$, *Phys. Rev. D* **92**, 033001 (2015), arXiv:1505.06568 [hep-ph].

[62] H.-R. He, X. Wan, and Y.-K. Wang, Anomalous $H \rightarrow ZZ \rightarrow 4\ell$ decay and its interference effects on gluon-gluon contribution at the LHC, *Chin. Phys. C* **44**, 123101 (2020), arXiv:1902.04756 [hep-ph].

[63] Y. Gao, A. V. Gritsan, Z. Guo, K. Melnikov, M. Schulze, and N. V. Tran, Spin Determination of Single-Produced Resonances at Hadron Colliders, *Phys. Rev. D* **81**, 075022 (2010), arXiv:1001.3396 [hep-ph].

[64] S. Bolognesi, Y. Gao, A. V. Gritsan, K. Melnikov, M. Schulze, N. V. Tran, and A. Whitbeck, On the spin and parity of a single-produced resonance at the LHC, *Phys. Rev. D* **86**, 095031 (2012), arXiv:1208.4018 [hep-ph].

[65] L. Cappiello, O. Cata, G. D'Ambrosio, and D.-N. Gao, $K^+ \rightarrow pi^+ pi^0 e^+ e^-$: a novel short-distance probe, *Eur. Phys. J. C* **72**, 1872 (2012), [Erratum: *Eur. Phys. J. C* 72, 2208 (2012)], arXiv:1112.5184 [hep-ph].

[66] S. R. Gevorkyan and M. H. Misheva, Different approaches to calculate the $K^\pm \rightarrow \pi^\pm \pi^0 e^+ e^-$ decay width, *Eur. Phys. J. C* **74**, 2860 (2014), arXiv:1403.1053 [hep-ph].

[67] R. Mertig, M. Bohm, and A. Denner, FEYN CALC: Computer algebraic calculation of Feynman amplitudes, *Comput. Phys. Commun.* **64**, 345 (1991).

[68] V. Shtabovenko, R. Mertig, and F. Orellana, New Developments in FeynCalc 9.0, *Comput. Phys. Commun.* **207**, 432 (2016), arXiv:1601.01167 [hep-ph].

[69] V. Shtabovenko, R. Mertig, and F. Orellana, FeynCalc 9.3: New features and improvements, *Comput. Phys. Commun.* **256**, 107478 (2020), arXiv:2001.04407 [hep-ph].

[70] R. L. Workman *et al.* (Particle Data Group), Review of Particle Physics, *PTEP* **2022**, 083C01 (2022).

[71] S. J. Lee, M. Park, and Z. Qian, Probing unitarity violation in the tail of the off-shell Higgs boson in $V_L V_L$ mode, *Phys. Rev. D* **100**, 011702 (2019), arXiv:1812.02679 [hep-ph].

[72] A. Bredenstein, A. Denner, S. Dittmaier, and M. M. Weber, Precise predictions for the Higgs-boson decay $H \rightarrow WW/ZZ \rightarrow 4$ leptons, *Phys. Rev. D* **74**, 013004 (2006), arXiv:hep-ph/0604011.

[73] A. Bredenstein, A. Denner, S. Dittmaier, and M. M. Weber, Precision calculations for the Higgs decays $H \rightarrow ZZ/WW \rightarrow 4$ leptons, *Nucl. Phys. B Proc. Suppl.* **160**, 131 (2006), arXiv:hep-ph/0607060.

[74] A. Bredenstein, A. Denner, S. Dittmaier, and M. M. Weber, Radiative corrections to the semileptonic and hadronic Higgs-boson decays $H \rightarrow WW/ZZ \rightarrow 4$ fermions, *JHEP* **02**, 080, arXiv:hep-ph/0611234.

[75] L. Altenkamp, S. Dittmaier, and H. Rzehak, Renormalization schemes for the Two-Higgs-Doublet Model and applications to $h \rightarrow WW/ZZ \rightarrow 4$ fermions, *JHEP* **09**, 134, arXiv:1704.02645 [hep-ph].

[76] L. Altenkamp, S. Dittmaier, and H. Rzehak, Precision calculations for $h \rightarrow WW/ZZ \rightarrow 4$ fermions in the Two-Higgs-Doublet Model with Prophecy4f, *JHEP* **03**, 110, arXiv:1710.07598 [hep-ph].

[77] L. Altenkamp, M. Boggia, and S. Dittmaier, Precision calculations for $h \rightarrow WW/ZZ \rightarrow 4$ fermions in a Singlet Extension of the Standard Model with Prophecy4f, *JHEP* **04**, 062, arXiv:1801.07291 [hep-ph].

[78] A. I. Hernández-Juárez, Mathematica code for $h^* \rightarrow zz \rightarrow \bar{\ell}_1 \ell_1 \bar{\ell}_2 \ell_2$ analysis, <https://gitlab.com/alaban792/off-shell-higgs-decay-to-4-leptons>, accessed: 2024-04-05.

[79] J. Alwall, R. Frederix, S. Frixione, V. Hirschi, F. Maltoni, O. Mattelaer, H. S. Shao, T. Stelzer, P. Torrielli, and M. Zaro, The automated computation of tree-level and next-to-leading order differential cross sections, and their matching to parton shower simulations, *JHEP* **07**, 079, arXiv:1405.0301 [hep-ph].

[80] C. Degrande, C. Duhr, B. Fuks, D. Grellscheid, O. Mattelaer, and T. Reiter, UFO - The Universal FeynRules Output, *Comput. Phys. Commun.* **183**, 1201 (2012), arXiv:1108.2040 [hep-ph].

[81] N. D. Christensen and C. Duhr, FeynRules - Feynman rules made easy, *Comput. Phys. Commun.* **180**, 1614 (2009), arXiv:0806.4194 [hep-ph].

[82] A. Denner, S. Dittmaier, M. Roth, and L. H. Wieders, Electroweak corrections to charged-current $e^+ e^- \rightarrow 4$ fermion processes: Technical details and further results, *Nucl. Phys. B* **724**, 247 (2005), [Erratum: *Nucl. Phys. B* 854, 504–507 (2012)], arXiv:hep-ph/0505042.

[83] T. Hahn and M. Perez-Victoria, Automatized one loop calculations in four-dimensions and D-dimensions, *Comput. Phys. Commun.* **118**, 153 (1999), arXiv:hep-ph/9807565.

[84] U. Baur and E. L. Berger, Probing the weak boson sector in $Z\gamma$ production at hadron colliders, *Phys. Rev. D* **47**, 4889 (1993).

[85] G. J. Gounaris, J. Layssac, and F. M. Renard, Signatures of the anomalous $Z\gamma$ and ZZ production at the lepton and hadron colliders, *Phys. Rev. D* **61**, 073013 (2000), arXiv:hep-ph/9910395.

- [86] U. Baur and D. Zeppenfeld, Unitarity Constraints on the Electroweak Three Vector Boson Vertices, *Phys. Lett. B* **201**, 383 (1988).
- [87] J. A. Aguilar-Saavedra, Tripartite entanglement in $H \rightarrow ZZ, WW$ decays, (2024), arXiv:2403.13942 [hep-ph].
- [88] K. Hagiwara and M. L. Stong, Probing the scalar sector in $e+ e- \rightarrow f \bar{f}$ H , *Z. Phys. C* **62**, 99 (1994), arXiv:hep-ph/9309248.
- [89] C. Li and G. Moortgat-Pick, Determination of CP-violating HZZ interaction with polarised beams at the ILC, (2024), arXiv:2405.08494 [hep-ph].
- [90] K. Abe *et al.* (SLD), Precise measurement of the left-right cross-section asymmetry in Z boson production by $e+ e-$ collisions, *Phys. Rev. Lett.* **73**, 25 (1994), arXiv:hep-ex/9404001.
- [91] S. Narita, *Measurement of the polarized forward - backward asymmetry of s quarks at SLD*, Ph.D. thesis, Tohoku U. (1998).
- [92] N. Cabibbo and A. Maksymowicz, Angular Correlations in $Ke-4$ Decays and Determination of Low-Energy pi-pi Phase Shifts, *Phys. Rev.* **137**, B438 (1965), [Erratum: *Phys. Rev.* 168, 1926 (1968)].
- [93] A. Pais and S. B. Treiman, Pion Phase-Shift Information from $K_{\ell 4}$ Decays, *Phys. Rev.* **168**, 1858 (1968).
- [94] E. Byckling and K. Kajantie, Kinematic separation of three-particle channels in counter experiments, *Nucl. Phys. B* **14**, 355 (1969).
- [95] E. Byckling and K. Kajantie, Reductions of the phase-space integral in terms of simpler processes, *Phys. Rev.* **187**, 2008 (1969).
- [96] E. Byckling and K. Kajantie, N-particle phase space in terms of invariant momentum transfers, *Nucl. Phys. B* **9**, 568 (1969).
- [97] E. Byckling and K. Kajantie, COUNTER EXPERIMENTS FOR THREE-PARTICLE FINAL STATES, (1969).
- [98] E. Byckling and K. Kajantie, *Particle Kinematics: (Chapters I-VI, X)* (University of Jyvaskyla, Jyvaskyla, Finland, 1971).
- [99] H.-Y. Cheng, C.-Y. Cheung, W. Dimm, G.-L. Lin, Y. C. Lin, T.-M. Yan, and H.-L. Yu, Heavy quark and chiral symmetry predictions for semileptonic decays $\bar{B} \rightarrow D (D^*) \pi$ lepton $\bar{\nu}$, *Phys. Rev. D* **48**, 3204 (1993), arXiv:hep-ph/9305340.